Probiotics and Antimicrobial Proteins (2026) 18:4540–4568
https://doi.org/10.1007/s12602-025-10760-7

RESEARCH

Pangenome Analysis and Genome-Guided Probiotic Evaluation of Cyclic Dipeptides Producing *Levilactobacillus brevis* DY55bre Strain from a Lactic Acid Fermented Shalgam to Assess Its Metabolic, Probiotic Potentials, and Cytotoxic Effects on Colorectal Cancer Cells

Ahmet E. Yetiman[1] · Mehmet Horzum[1,2] · Ertan Kanbur[3] · Mehmet Çadir[4] · Dilek Bahar[5] · Şerife Gürbüz[5] · Melisa Z. Karaman[6] · Özkan Fidan[6] · Murat Kaya[7] · Sevda Yetiman[8] · Mahmut Doğan[1] · Mikail Akbulut[9]

Received: 10 May 2025 / Accepted: 29 August 2025 / Published online: 1 October 2025

Abstract

This study investigates the genetic, metabolic, and probiotic characteristics of *Levilactobacillus brevis* DY55bre, a strain isolated from the traditional Turkish fermented beverage, shalgam. Whole-genome sequencing revealed a circular genome of 2.485 Mb with a GC content of 45.72%, predicted 2791 genes, and multiple CRISPR-Cas systems. Pangenome analysis demonstrated an open structure, with 18.9% core genes and 103 strain-specific genes, highlighting its genetic diversity. The DY55bre exhibits heterofermentative carbohydrate metabolism due to the presence of the *araBAD* operon and the lack of 1-phosphofructokinase (*pfK*) and fructose-1,6-bisphosphate aldolase enzymes. Probiotic evaluation revealed firm survival under simulated gastrointestinal conditions, including resistance to acidic pH (as low as 3.0) and bile salts (up to 1%), along with significant adhesion to intestinal epithelial cell lines (HT29;59.3%, Caco-2;87%, and DLD-1;60.8%). The strain exhibited high auto-aggregation (84.55%) and cell surface hydrophobicity (56.69%), essential for gut colonization. Safety assessments confirmed its non-hemolytic nature and absence of horizontally acquired antibiotic resistance genes. Notably, GC-MS analysis identified bioactive cyclic dipeptides, Cyclo(D-Phe-L-Pro) and Cyclo(L-Leu-L-Pro), which demonstrated cytotoxic effects against colorectal cancer cell lines, with IC50 values of 7.71 mg/mL for HT29 and 3.19 mg/mL for DLD-1. The cell-free supernatant exhibited antimicrobial activity against pathogens, likely due to the synergistic effects of cyclic dipeptides, organic acids, and other metabolites. Antioxidant assays revealed significant $ABTS^{+}$ (76.63%) and DPPH (34.25%) radical scavenging activities, while cholesterol assimilation tests showed a 27.29% reduction. These findings position the DY55bre as a promising candidate for functional foods, nutraceuticals, and therapeutic applications, warranting further in vivo validation.

Keywords Cholesterol · Antimicrobial activity · Pangenome · Probiotic · Anticancer · *Levilactobacillus*

✉ Ahmet E. Yetiman
ahmetyetiman@erciyes.edu.tr

[1] Food Engineering Department, Faculty of Engineering, Erciyes University, 38030 Kayseri, Turkey

[2] Food Engineering Department, Graduate School of Natural and Applied Sciences, Erciyes University, 38030 Kayseri, Turkey

[3] Department of Immunology, Faculty of Medicine, Kırşehir Ahi Evran University Bağlarbaşı Campus, 40100 Kırşehir, Turkey

[4] Technology Research and Application Center, Erciyes University, Kayseri 38030, Turkey

[5] Genkök Genome and Stem Cell Center, Erciyes University, 38030 Kayseri, Turkey

[6] Department of Bioengineering, Faculty of Life and Natural Sciences, Abdullah Gül University, Kayseri 38080, Turkey

[7] Food Technology Department, Safiye Cikrikcioglu Vocational School, Kayseri University, Kayseri 38000, Turkey

[8] ERNAM, Erciyes University Nanotechnology Application and Research Center, Kayseri 38039, Turkey

[9] Department of Biology, Faculty of Science, Erciyes University, 38030 Kayseri, Turkey

Introduction

Levilactobacillus brevis (*Lvb. brevis*) belongs to the group of lactic acid bacteria (LAB), characterized by their lack of catalase activity, inability to form spores, and absence of motility. They typically have a rod or coccus shape. *Lvb. brevis* exhibits optimal growth at a temperature of 30 °C and a pH range of 4 to 6 [1]. It is an obligate heterofermentative that can generate lactic acid, carbon dioxide, and ethanol or acetic acid [2]. *Lvb. brevis* has been isolated from various sources, including cheese, Korean kimchi, beer, human gut, pig feces, fruit fly, sourdough, sheep rumen, shalgam, and cucumber pickles [3–5].

Strains of *Lvb. brevis* have been described to exhibit beneficial functions as probiotics, such as maintaining the balance of gut microbiota [6], regulating inflammatory and immune responses [7], enhancing skin health [8], and combating obesity [9]. *Lvb. brevis* members also have been reported to demonstrate high efficiency in synthesizing γ-aminobutyric acid (GABA), which offers various health advantages [10, 11]. Besides, *Lvb. brevis* cells or their metabolites may exhibit antiviral activity [12, 13]. Moreover, certain LAB strains associated with fermentation have considerable industrial interest due to a variety of biotechnological applications, such as functional starter cultures, adjuncts, probiotics, or components of simplified custom-made microbial communities to enhance the safety, health-related properties, and sensory quality of fermented foods [14]. Due to those presumed characteristics, the majority of *Lvb. brevis* strains have been acknowledged as generally recognized as safe (GRAS) and/or presumably qualified as safe (QPS) [15, 16].

Every strain of probiotics has distinct and exceptional characteristics, encouraging research for new probiotics or potential biotech strains. Their biological functions are particular to each strain, and it is impossible to generalize these features to other strains of the same species [17]. Hence, it is crucial to ascertain these characteristics by conducting physiological and metabolic testing and using functional genomics methods when a remarkable new strain is acquired in any habitat [13, 18]. Shalgam was characterized by a reddish color, sour-soft taste, and fuzzy appearance [19]. Besides, it has been claimed that it has presumptive health benefits versus several health risks and diseases because the content of LAB exists in its microbiota [18, 20]. *Lactiplantibacillus plantarum* and *Lactocaseibacillus paracasei* were reported to be prevalent in its microbial distribution [21]. Other species known in the shalgam microbiota include *Lbs. casei*, *Lvb. brevis*, *Lvb. parabrevis*, *Llb. buchneri*, *Lmb. fermentum*, *Lmb. reuteri*, *Lpb. pentosus*, *Lb. delbrueckii* subsp. *delbrueckii*, *Lb. helveticus*, *Lb. acidophilus*, *Lvb. gasseri*, *Pediococcus* spp., *Leu. mesenteroides* subsp. *mesenteroides*, *Leu. mesenteroides* subsp. *mesenteroides/dextranicum*, and *Leu. mesenteroides* subsp. *cremoris* [20].

The present study aimed to appraise the genetic, physiological, and metabolic traits of *Lvb. brevis* DY55bre using functional genomics techniques, with a particular focus on its biotechnological and probiotic potential. The genome of the DY55bre strain was sequenced with Illumina Novaseq. To our knowledge, no studies have been related to shalgam originating from *Lvb. brevis* strains, according to PubMed search results as of 9 May 2025. The majority of comparative studies of *Lvb. brevis* have been focused on its association with breweries or pickling processes [22–26]. Unlike previous studies on *Lvb. brevis*, this study attempted to provide insight into its carbohydrate metabolism and safety assessment, along with genome-guided characterization of probiotic features and comparative analysis of probiotic genes across other *Lvb. brevis* strains. Moreover, we detected anticancer properties most probably due to cyclic dipeptides of Cyclo(D-Phe-L-Pro) and Cyclo(L-Leu-L-Pro) produced by the DY55bre. In this respect, it is possible to claim that this study is one of the first to investigate the probiogenomic traits and functional characterization of the *Lvb. brevis* strain isolated from shalgam.

Materials and Methods

Isolation and Growth Conditions of DY55bre

The *Lvb. brevis* strain DY55bre was isolated from a commercially available Turkish fermented shalgam juice (pH: 3.01) sourced from a local producer (Doktorum Yılmaz) in Adana, Türkiye. A 10 mL aliquot of the sample was diluted with 90 mL of sterile physiological saline solution (0.85%) and then homogenized for 1 min using a high-speed vortex mixer (MS-3 Basic, IKA-Werke GmbH, Staufen, Germany). Subsequently, serial decimal dilutions were prepared from the suspension, and 100 µL of each dilution was applied onto MRS agar (Merck GmbH, Darmstadt, Germany). The plates were incubated at 30 °C for 5 days in an oxygen-free environment. The isolate known as DY55bre was selected from a dilution of 10^{-5} and underwent two rounds of colony purification. Subsequently, the pure DY55bre isolate was exposed to a catalase test and Gram staining. The DY55bre cryo stocks were produced using MRS broth (Merck) supplemented with 25% glycerol and kept at −80 °C.

DNA Isolation, Identification, Sequencing, and Assembly

First, a *Lvb. brevis* DY55bre cryo culture was subcultured twice in MRS broth (Merck), then anaerobically kept at 37

°C for 24 h. A 1 mL fresh culture was pipetted inside a sterile microcentrifuge tube (2 mL) and centrifuged for 10 min at 4 °C at 6000 × g. Then, total DNA was extracted from the cell pellet using the PureLink Genomic DNA Mini Kit (Invitrogen, Thermo-Fisher Scientific, Carlsbad, CA, USA) based on the manufacturer's suggestions for Gram-positive bacteria. We employed the Qubit 3.0 fluorometer (Invitrogen, Thermo-Fisher Scientific, Carlsbad, CA, USA) and Agilent 5400 Fragment Analyzer to analyze the gDNA content, integrity, and purity of the DY55bre sample. The acquired gDNA was then used to generate a DNA library using the Nextera XT DNA Library Preparation Kit (Illumina, USA) before being transported to the next-generation sequencing platform. The impurities in the library were eliminated using the AMPure XP bead (Beckman Coulter, UK) manufacturer's protocols. Whole genome sequencing was conducted using the NovaSeq 6000 platform with 2 × 150 bp pair-end (PE) chemistry. After sequencing, the whole genome data were retrieved in "fastq.gz" format. Trimmomatic software (v0.36) was used via Kbase to trim adapter and barcode sequences from genome data [27]. Later, trimmed raw data were assembled using SPAdes v3.13.0 with a CheckM completeness score of 100 as the genome quality parameter [28].

Bioinformatic Analyses

The NCBI Prokaryotic Genome Annotation Pipeline (PGAP) was used to accomplish genome annotation [29]. RASTtk and BV-BRC annotations were also performed for comparison with PGAP [30, 31]. The genome data package used during this study was downloaded from the NCBI website (Taxon ID: 1580). BRIG v0.95 was used to build a BLAST Ring Image of the genome of the DY55bre strain and other comparable *Lvb. brevis* strains [32]. Prior to pangenome analysis, all *Lvb. brevis* genomes used in this study were merged into a single contig and annotated using Prokka (v.1.14.5) [33]. Pangenome analysis was conducted via Pan-genome Explorer using the PanACoTA comparative genomics tool with an 80% minimum identity [34, 35]. The Fast ANI technique calculated the average nucleotide identity values (fastANI) of the DY55bre and other analogous *Lvb. brevis* strains [36]. The dbCAN3 meta server was employed to predict CAZYmes [37]. Besides, for comparison purposes, the metabolic pathways of *Lvb. brevis* DY55bre were predicted using BlastKOALA for scanning against the KEGG database. A resistome screening was performed by examining the DY55bre strain's whole genome sequence using BV-BRC and KEGG databases. The protein-coding sequences of antibiotic resistance-associated genes were screened against the NCBI-non-redundant protein (NR) database using protein-BLAST to detect horizontally transmitted genes. When a gene's homologous protein was found to be at least 80% identical to a bacterium other than *Lvb. brevis*, it was considered to be affected by horizontal gene transfer. The CRISPR structures present in the genome of DY55bre were examined with CRISPRCasFinder [38]. The R Studio environment was employed for data visualization, particularly for forming heatmaps [39]. The metabolic overview of putative carbohydrate metabolism was depicted using PathVisio V.3.30 [40]. Last, secondary metabolites and related gene clusters of interest were successfully predicted using antiSMASH version 7.1.0 [41]. The genome and plasmid sequences have been submitted to the NCBI under the accession numbers (BioSample: SAMN37828895) CP136801 and CP136802, respectively.

Probiotic Characteristics Analysis

The following experiments were done to establish the probiotic qualities of the DY55bre: β-haemolysis, in vitro mimicking of gastrointestinal digestion, cell surface hydrophobicity, cellular auto-aggregation testing, and antibacterial activity assay against different pathogens. The DY55bre's β-hemolytic activity was tested on a Mueller-Hinton plate containing 5% sheep blood (Aklab, Erzurum, Türkiye). The isolate was streaked on Columbia agar and then incubated at 37 °C for 48 h under anaerobic conditions. To examine the DY55bre's reaction to the gastrointestinal tract, INFOGEST in vitro static gastric digestion simulation was carried out as reported by Brodkorb et al. [42] with minor modifications described by Yetiman [17]. In this simulation, no carrier food environment was employed; ultra-pure water was used instead. The cell surface hydrophobicity and auto-aggregation experiments were implemented following Krausova et al. [43]. The agar well diffusion technique was used to examine the bactericidal activity of the cell-free supernatant of DY55bre. The cell-free supernatant (40 mL) from bacterial cells grown for 48 h was freeze-dried (Christ, Alpha 2–4 LSCplus, Germany) and resuspended in 5 mL of sterile ultra-pure H_2O. It was subsequently tested against *Escherichia coli* O157:H7 (ATCC 43895), *Bacillus cereus* (ATCC 33019), *Salmonella enterica* sv. typhimurium (ATCC 14028), *Proteus mirabilis* (ATCC 29906), and *Enterobacter cloacae* (ATCC 13047) from the culture collection of Erciyes University Food Engineering Department. All steps of the antimicrobial activity assay were performed according to Ozturk et al. [44].

Adhesion Assay in HT29, Caco-2, and DLD-1 Cell Lines and Image Acquisition

The adhesion assay was performed according to Song et al. with some modifications [45]. HT29, Caco-2, and DLD-1 cells, derived from human colon adenocarcinoma, were obtained from the GENKÖK (Erciyes University Genome and Stem Cell Center) to conduct an adhesion assay. For

cell cultures, HT29 cell line was cultured with hDMEM; Caco-2 cell line was cultured with eMEM; and DLD-1 cell Line was cultured with RPMI mediums with 10% FBS, 1% L-glutamine, and 1% penicillin-streptomycin in a humidified 37 °C CO_2 incubator inside a 25 cm^2 cell growth area containing sterile cell culture flasks (NEST Biotechnology, Wuxi, Jiangsu, China). To test the adhesion capacity of the DY55bre in HT29, Caco-2, and DLD-1 cells, the cells were cultivated at a concentration of 10^5 cells/well on 24-well culture plates with their respective media and incubated for 24 h. Subsequently, 100 µL of DY55bre cells (1×10^9 CFU/well) was added to the adhered cells and incubated for 2 h. Later, wells were washed three times with PBS solution containing 0.5% Triton X-100 (Roche, Germany) to remove bacterial cells. The DY55bre's adhesion ability to the employed cell lines was assessed via a plate counting method on MRS agar and determined as follows:

$$Adhesion\ ability(\%) = 100 - \left(\frac{The\ number\ of\ bacteria\ after\ incubation\ (CFU/\mathrm{mL})}{The\ number\ of\ bacteria\ before\ incubation\ (CFU/mL)} \times 100\right)$$

In addition, cells were grown in 35-mm cell culture plates (µ-dish, Ibidi, Germany) with their own culture media for image acquisition. The cells (10^5) were co-cultivated with 10^9 CFU/mL of DY55bre cells and incubated for 2 h at 37 °C in a 5% CO_2 atmosphere. Later, cells were fixed using 2.5% glutaraldehyde for 10 min, plates were washed, and Gram staining was applied for microscopic examination.

Determination of Anti-proliferative Effects Using CCK-8 Assay

The cytotoxic effects of bacterial cell-free supernatants were assessed in the HT-29 and DLD-1 human colon cancer cell lines. Cell viability analysis was conducted via the colorimetric assay of the CCK-8 (Cell Counting Kit-8, MedChemExpress, NJ, USA). Cells were seeded on 96-well cell culture plates at a density of 1×10^4 cells per well and allowed to adhere for 24 h. After adhesion, cells were subjected to various amounts of bacterial supernatants. Culture-free blank MRS broth was used as a negative control, which ensured reliable comparisons. Following 24 h of incubation with the test samples, 10 µL of CCK-8 reagent was added to each well, and the cells were further incubated at 37 °C for 4 h. Cell viability was evaluated by measuring absorbance at 450 nm using a microplate reader (MultiSkan Skyhigh, Thermo-Fisher Scientific, USA). Afterward, absorbance values were assessed by generating dose-response curves. IC_{50} values (half-maximal inhibitory concentration) and cellular viability graphs were calculated utilizing GraphPad Prism (Boston, MA, USA) software [46].

Analysis of Cell-Free Supernatants with GC-MS

The freeze-dried CFS of DY55bre was chemically derivatized for GC-MS analysis [47]. Briefly, 50 µL of MTBSTFA (N-tert-butyldimethylsilyl-N-methyltrifluoroacetamide, Sigma, Germany) containing 500 µL of DMSO and 1% t-butyldimethylchlorosilane (TBDMS-Cl) was added as a catalyst to the freeze-dried CFS samples. The tubes were sealed and Heated for 1 h at 80 °C on a dry block. After cooling, the samples were centrifuged at 5000 × g for 15 min in a microfuge to precipitate any salt or particulate material. The clear reaction supernatants were transferred to 0.5-mL autosampler vials for GC-MS analyses. This process added a tBDMS group (+ 114) to each -COOH, $-NH_2$, -SH, $-SO_2H$, and -OH functional group. In the case of pyruvic acid, derivatization of the -C = O group also occurred. Afterward, GC-MS analysis was performed on a Shimadzu GC-MS-QP2010 Ultra gas chromatograph mass spectrometer (Japan). The chromatographic separation was achieved on an Rtx-5 MS capillary column (30.0 m × 0.25 mm × 0.25 µm; Restek GmbH, Germany) using ultrapure helium (purity ≥ 99.999%) as carrier gas with a flow rate of 2.00 mL/min. The column oven was initially Held at 40 °C for 1 min, then increased to 100 °C for 1 min at the rate of 2 °C/min, and then increased to 270 °C for 5 min at the rate of 2 °C/min. The temperature of the injector was Held at 280 °C in splitless mode. And the volume of injection was 2 µL. The interface and ion source temperatures were 280 and 300 °C, respectively. Selective ion monitoring mode (SCAN) was applied for the quantitative analysis. The solvent delay was set as 5 min. These procedures were applied to non-culture-containing MRS broth as a blank measurement. Moreover, all derivatization treatments and GC-MS analyses were carried out on samples dissolved in acetonitrile instead of DMSO.

Antioxidant Activity Assays

DDPH (2,2-diphenyl-1-picrylhydrazyl) and ABTS (2,2-azinobis (3-ethylbenzothiazoline-6-sulfonic acid) techniques were used to assess the antioxidant activity of the DY55bre. Cell-free supernatant (CFS) was extracted from MRS broth by centrifugation at 3500 rpm for 15 min. The DPPH scavenging activity was determined using a modified version of the method described by Öztürk et al. [44]. Two milliliters of freshly produced 0.2 mM DPPH was added to 1 mL of four times diluted CFS to make the reaction mixture. At 25 °C, the mixture was incubated in the dark for 30 min. The mixture was

centrifuged at 5000 rpm before being measured at 520 nm with five repetitions. The blank control consists of dH_2O and DPPH solutions. The scavenging activity $\% = (1 - A_{test}/A_{blank}) \times 100$ formula was used to calculate DPPH scavenging activity (*A* stands for absorbance).

ABTS assay was fulfilled according to Yetiman et al. [13]. ABTS (7 mM) was dissolved in water. After that, the ABTS stock solution was combined with 2.45 mM potassium persulfate (final concentration) to create radical cation ($ABTS^+$), and the mixture was kept in the dark for 16 h at 25 °C before use. Before implementation, the $ABTS^+$ solution was diluted with phosphate buffer (pH: 7.2) to achieve an absorbance of 0.700 ± 0.03 at 734 nm. Similarly, the CFS was diluted four times in phosphate buffer (pH: 7.2). After that, 40 µL of CFS was added to 4 mL of $ABTS^+$ solution, the mix was left in the dark for 5 min, and the absorbance was measured five times. Phosphate buffer (pH: 7.2) was utilized as a blank and control. The ascorbic acid standard curve (0–9 g/mL) was employed to predict the percentage of inhibition. Both analyses were conducted with ten replicates.

Cholesterol Assimilation Test

The O-phthaldehyde (OPA) technique, as described by Rudel and Morris [48], was used to examine cholesterol consumption by the DY55bre in MRS broth. The DY55bre was cultivated at 37 °C for 24 and 48 h in MRS broth (0.25% dextrose + 0.3% ox bile containing) supplemented with 100 ppm cholesterol (5-cholesten-3-ol (Sigma, Merck GmbH, Darmstadt, Germany), dissolved in 2-propanol). The cultures were centrifuged (3500 rpm, 15 min, 25 °C), and CFS was utilized to measure residual cholesterol. The CFS was mixed with 2 mL of KOH (50% w/v) and 3 mL of absolute ethanol, vortexed for 1 min, then Heated at 60 °C for 15 min. After cooling, the mixture was vortexed for 1 min with 3 mL dH_2O and 5 mL Hexane. Then, 2.5 mL of the Hexane phase was transferred to another glass tube and kept at 80 °C for evaporation. The residue was dissolved in 4 mL of OPA (0.5 mg/mL in glacial acetic acid) and incubated for 10 min at 25 °C. Later, 2 mL of H_2SO_4 (98%) was gently added and vortexed for 1 min before the solutions were incubated at 25 °C for 10 min, and absorbance was measured at 550 nm (Shimadzu UV-1800 UV/VIS spectrophotometer, Tokyo, Japan). The difference between the control (uninoculated MRS broth) and test samples was used to calculate cholesterol assimilation.

Results and Discussion

Genomic Features and ANI Comparison

The *Lvb. brevis* strain DY55bre genome incorporated 2791 genes, 2699 protein-coding sequences, 82 tRNA, 3 5S rRNA, 2 16S rRNA, 2 23S rRNA, 3 non-coding RNA, 4 CRISPR array regions, and 155 pseudogenes on a circular chromosome of 2,485,670 bp with a 45.72% GC ratio. The BLAST ring alignment of all *Lvb. brevis* genomes, including DY55bre, is depicted in Fig. 1, where variations between them can be recognized easily due to gaps in the genomes. Detecting genomic islands among these gaps is achievable due to the associated drop in GC content and the absence of similar islands in other strains. In general, integrases, insertion sequences, and transposases are found in and/or around these islands, indicating the presence of possibly horizontally transmitted genes [13]. Nucleotide statistics provide more evidence of genomic islands, including cumulative GC skew, GC% content, tetranucleotide frequencies, or codon use [49, 50]. Additionally, lactobacilli are generally regarded as low-GC organisms [51], and it was reported in a study by Brandt and Barrangou [52] that the mean GC content of lactobacilli was approximately 40.70%. It is possible to infer from these findings that *Lvb. brevis* has encountered less genomic drift.

The findings of the FastANI comparison between the DY55bre genome and the other analyzed genomes are shown in Fig. 2. Determining whether the genomes of the two species are regarded as identical relies on the ANI value surpassing 95% [53, 54]. The genome of *Lvb. brevis* DY55bre has been observed to be similar to the genomes of YSJ3 (99.09%), SA_C12 (98.97%), ATCC367 (98.96%), 100D8 (98.95%), KB290 (98.92%) Lb1595 (98.86%), SRCM101174 (98.85%), AG48 (98.84%), NSMJ23 (98.80%), and WK12 (98.76%) which were derived from pickle, silage, rye silage, commercial probiotic (fermented vegetable), hospital swab, food, sheep rumen, makgeolli, and kimchi, respectively (Fig. 2). The genetic divergence or similarities among the DY55bre genome and the genomes mentioned above can be attributed to variations or resemblances in the strain's ecological niche, evolutionary trajectories, and environmental circumstances [55]. Lactobacilli considered "allochthonous" originate from a different location and have no environmental or evolutionary connection to the habitat where they are found, unlike "autochthonous" species [56, 57]. However, the observed association and differences among the aforementioned different strains can be attributed to the free-living lifestyle of *Lvb. brevis*, facilitating the development of adaptive evolution in various ecological niches [17, 55]. Furthermore, lactobacilli can utilize host animals and insects as vectors or transient shelters for dispersal into diverse habitats [13]. This also validates the liberated lifestyle of *Lvb. brevis*.

CRISPR structures are extensively found in prokaryotes, serving as an adaptive immune system versus foreign invasive DNA [58]. Especially for lactic acid bacteria, it is possible to natively or externally engineer novel strains with better functional features using CRISPR-Cas systems

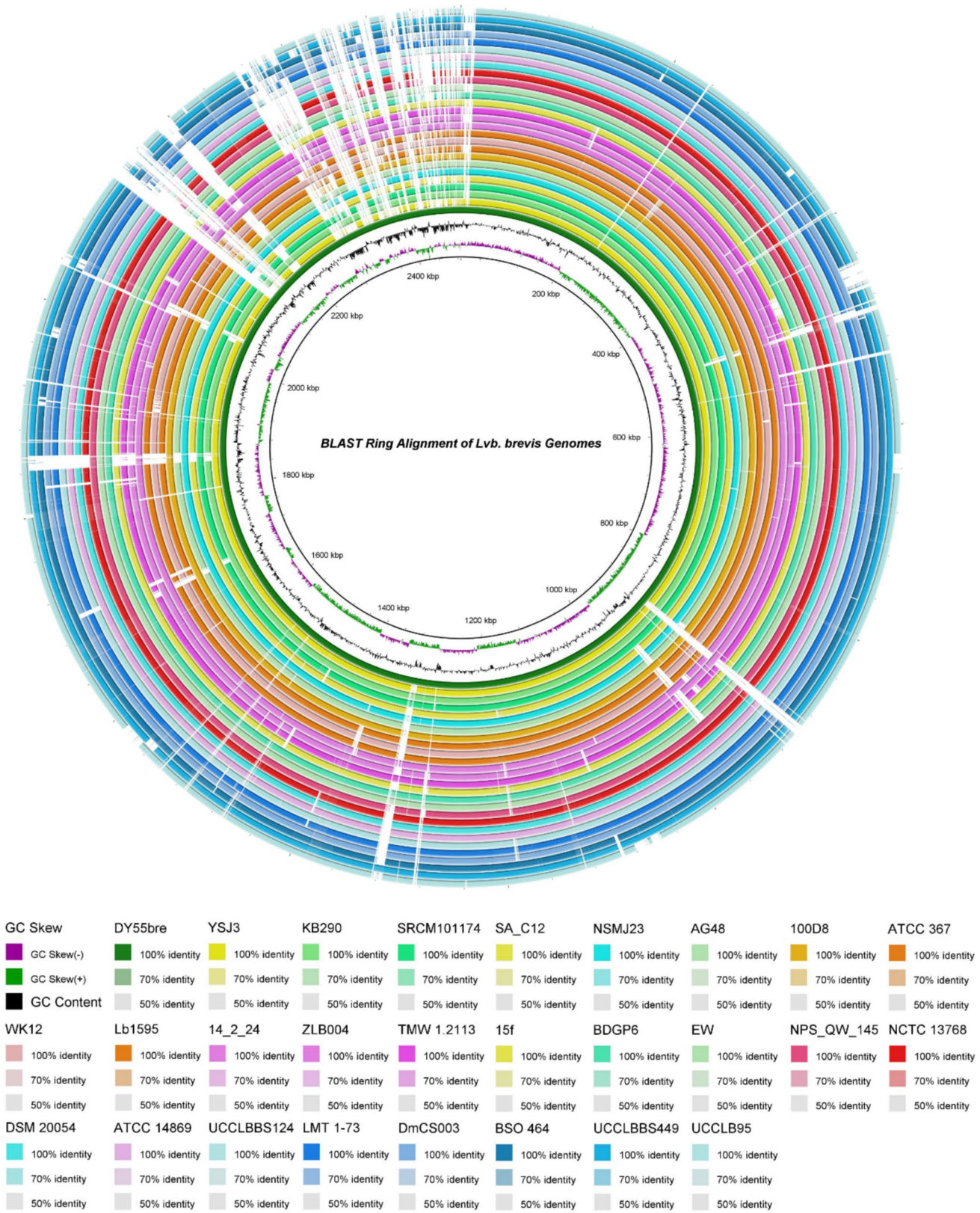

Fig. 1 BRIG alignment of *Lvb. brevis* genomes. The alignment began from the inner green ring (DY55bre) and extended to the outer blue ring (UCCLB95). The GC skew (+/−) of the DY55bre genome was displayed in the third inner circle, while the GC content was illustrated in the second inner circle. The genome size was also depicted in the first inner circle before the GC content

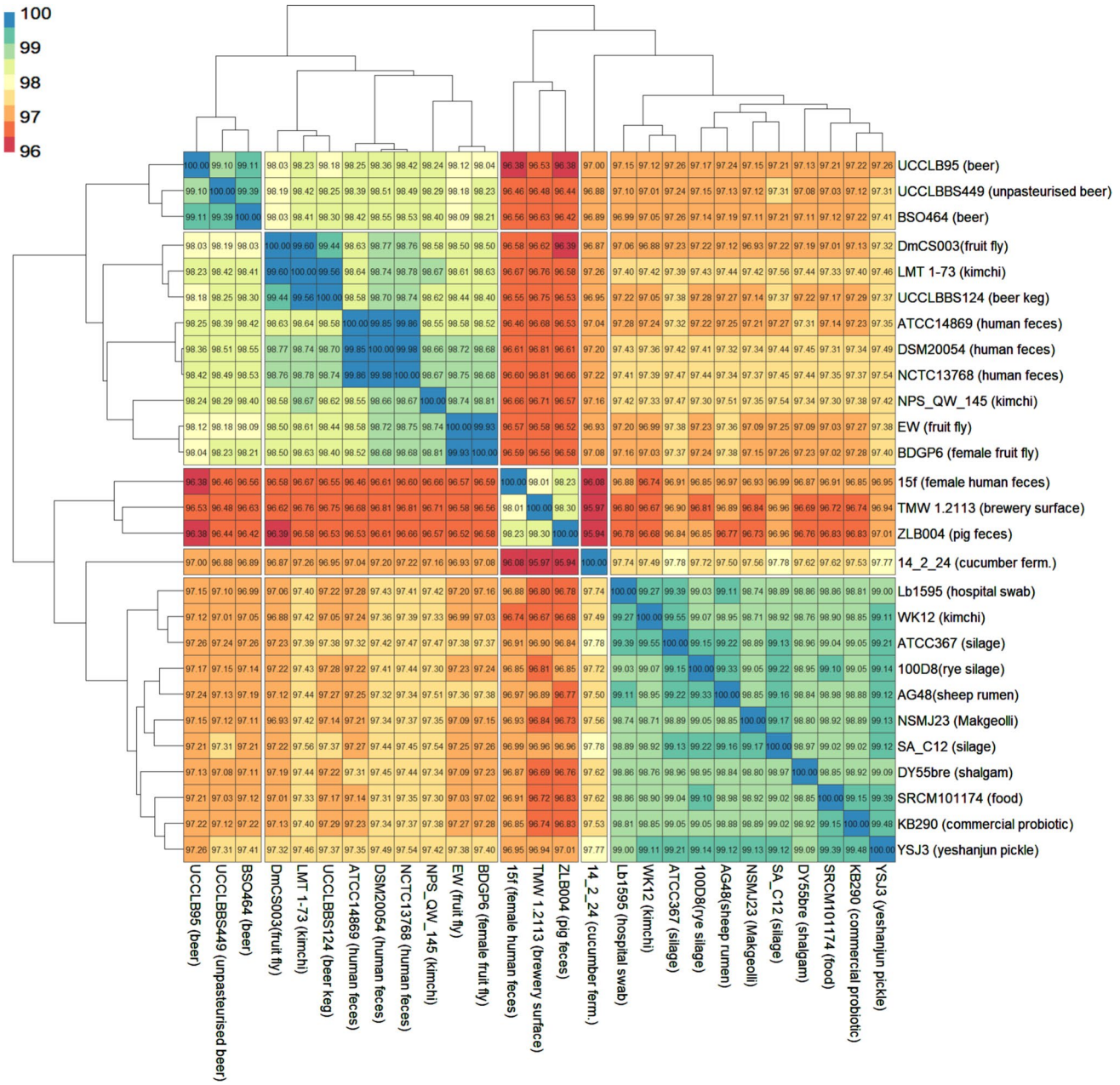

Fig. 2 Average nucleotide identity (ANI) phylogram of *Lvb. brevis* DY55bre and other well-known *Lvb. brevis* genomes. ANI values were calculated using the Fast ANI methodology, and the heatmap was created in the R environment

and associated molecular machines [59]. All genomes in the studied dataset have CRISPR spacers detected by the CRISPR structure screening. Cas genes were found in only three genomes: DY55bre, AG48, and EW. Based on previous studies, *Lvb. brevis* strains generally tend to have more than one CAS system, and the most common CAS systems are Type-II variants [60, 61]. Unlike prior research, the DY55bre genome harbors only one CAS system, Type-1E. The components of this system are the type signature Cas3 protein, the Type 1-E cascade complex consisting of Cas6e, Cse1, Cse2, Cas5, and Cas7, as well as the spacer-acquisition machinery proteins Cas1 and Cas2. Type 1E CAS systems are commonly associated with viral defense mechanisms [62], but they have also been used in rare cases for strain engineering attempts to acquire functional traits [63]. On the other hand, the DY55bre strain contains a total of 42 CRISPR spacers, several of which have been found on different *Lvb. brevis* genomes, including AG48 (25), ZLB004 (31), KB290 (1), and ATCC367 (10). Based on these findings, DY55bre has the potential to be

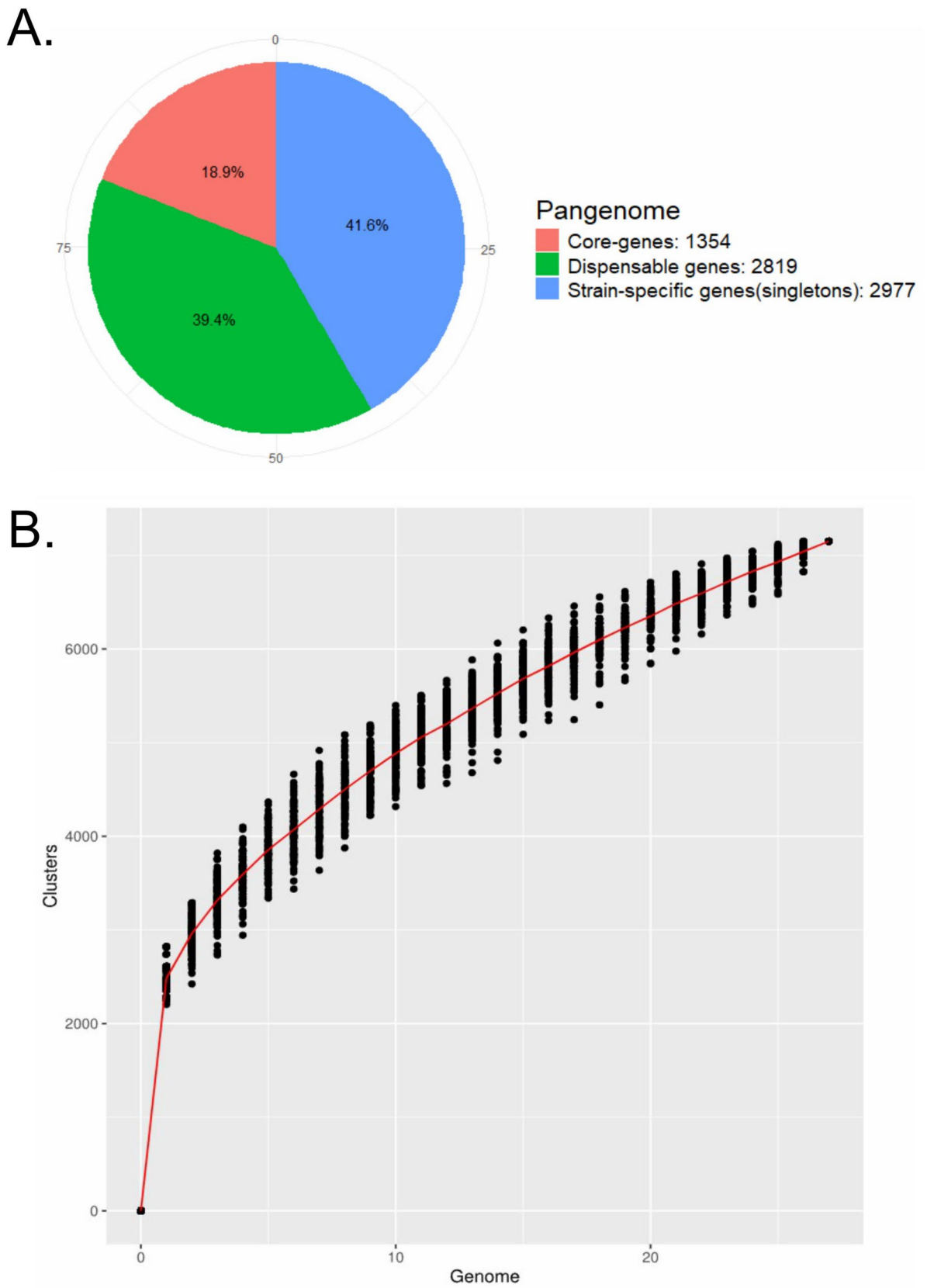
A.
0
25
50
75
18.9%
41.6%
39.4%
Pangenome
Core-genes: 1354
Dispensable genes: 2819
Strain-specific genes(singletons): 2977
B.
Clusters
0
2000
4000
6000
0
10
20
Genome

◂**Fig. 3** **A** Distribution of core genome and accessory genome. **B** The rarefaction curve, generated by the micropan R program, represents the cumulative count of gene clusters (pangenome) observed with an increasing number of genomes analyzed. Alpha value of 0.539438685569583 was obtained using the Heaps law approach proposed by Tettelin et al. (2008) [65]

exploited in strain engineering studies via its natural CAS system.

Pangenome Analysis

Pangenome analysis was also performed on the aforementioned genomes to estimate the complete gene pool of *Lvb. brevis*. The Pangenome analysis yielded a total of 7150 estimated genes (pangenome), which consisted of 1354 core genes (core genome), 2819 dispensable genes, and 2977 strain-specific (singletons) genes (Figs. 3A and 4). The core genome constitutes 18.9% of the pangenome and is typically associated with essential metabolic processes and primary functions necessary for maintaining the organism. In addition, they may possess genes that differentiate the species from others within the same genus [64]. Besides, the Pangenome curve had a logarithmic pattern and did not reach a plateau. The alpha value was calculated to be 0.539438685569583, as shown in Fig. 3B. According to the Heaps law technique suggested by Tettelin et al. [65], the Pangenome is considered open since it has an alpha value smaller than 1 and follows a logarithmic curve trend. Open pangenomes also enable widely spread species (like *E. coli*) to adapt to harsh settings by continuously acquiring genetic material from their surroundings. This makes it possible to achieve functional diversity [66].

The pangenome analysis revealed that "Replication, recombination, and repair" and "General function prediction only" are the most prevalent groups of COGs in the pangenome and core genome, respectively. Furthermore, it was established that the COG categories of "Transcription," "Replication, recombination, and repair," "Translation, ribosomal structure and biogenesis," and "Amino acid transport and metabolism" constituted the second, third, fourth, and fifth biggest segments of the core genome, respectively. In contrast, the COG categories of "Cell wall/membrane/envelope biogenesis," "General function prediction only," "Transcription," and "Amino acid transport and metabolism" accounted for the second, third, fourth, and fifth most significant sections of the pangenome, respectively. Moreover, the smallest core- and pangenome COG groupings were identified as "Cell motility" and "Intracellular trafficking, secretion, and vesicular transport" correspondingly. A detailed illustration of the frequency of core- and pangenome-associated COG categories is shown in Fig. 5. Clustered accessory genes are depicted in Fig. 6, indicating whether or not they are present in the analyzed genomes.

Among the 2977 strain-specific genes identified in the Pangenome, 103 are unique singletons associated with DY55bre. The COG categories of these singletons are summarized as follows: Five genes are specifically implicated in the regulation of the cell cycle, cell division, and chromosome partitioning. Five genes are specifically involved in nucleotide transport and metabolism, while 18 genes are associated with carbohydrate transport and metabolism. Eight genes participate in transcription, whereas 12 genes are engaged in replication, recombination, and repair. There are 12 genes Linked to cell wall, membrane, and envelope biogenesis; 13 genes related to inorganic ion transport and metabolism; and 2 genes involved in the biosynthesis, transport, and catabolism of secondary metabolites. Seventeen genes are solely implicated in general function prediction. Seven genes exhibit unknown functions, while two genes are associated with signal transduction mechanisms. Moreover, the gene numbers of COG functional categories belonging to strain-specific genes were compared with each other in a heatmap (Fig. 7). A significant proportion of singleton genes, often exceeding 70% in various strains, are annotated as hypothetical despite being classified within a COG category. This is consistent with previous findings that singleton genes are frequently poorly characterized, possibly due to their recent acquisition or rapid evolution [67, 68]. Some singleton genes may represent remnants of ancestral genes that have been lost in other strains due to functional redundancy or changes in selective pressures. As a result, these genes persist as singletons in only one or a few genomes, often with unknown or hypothetical functions [69]. Singleton genes frequently arise from horizontal gene transfer events, involving the acquisition of genetic material from unrelated organisms. This process incorporates novel genes into a genome, many of which may be specific to an individual strain and not yet established within the population. These genes commonly encode functions associated with adaptation, including antibiotic resistance, virulence, or specialized metabolism, and are typically categorized under "Replication, recombination and repair" (L) or "Cell wall/membrane/envelope biogenesis" (M) [67, 68, 70]. The detected numbers of orthologous groups (COG) of individual protein-coding sequences in the *Lvb. brevis* DY55bre genome are summarized in Fig. 8.

Furthermore, a comprehensive presence/absence analysis of strain-specific functional genes (Table S2) demonstrates that DY55bre possesses a suite of unique genes absent in the closely related genomes YSJ3 and SA_C12 based on Fast ANI results. Specifically, DY55bre encodes S-layer proteins and multiple biofilm regulatory proteins (e.g., CLUSTER1984 [S-layer protein], CLUSTER6558 [Biofilm regulatory protein A], and CLUSTER6382 [Biofilm

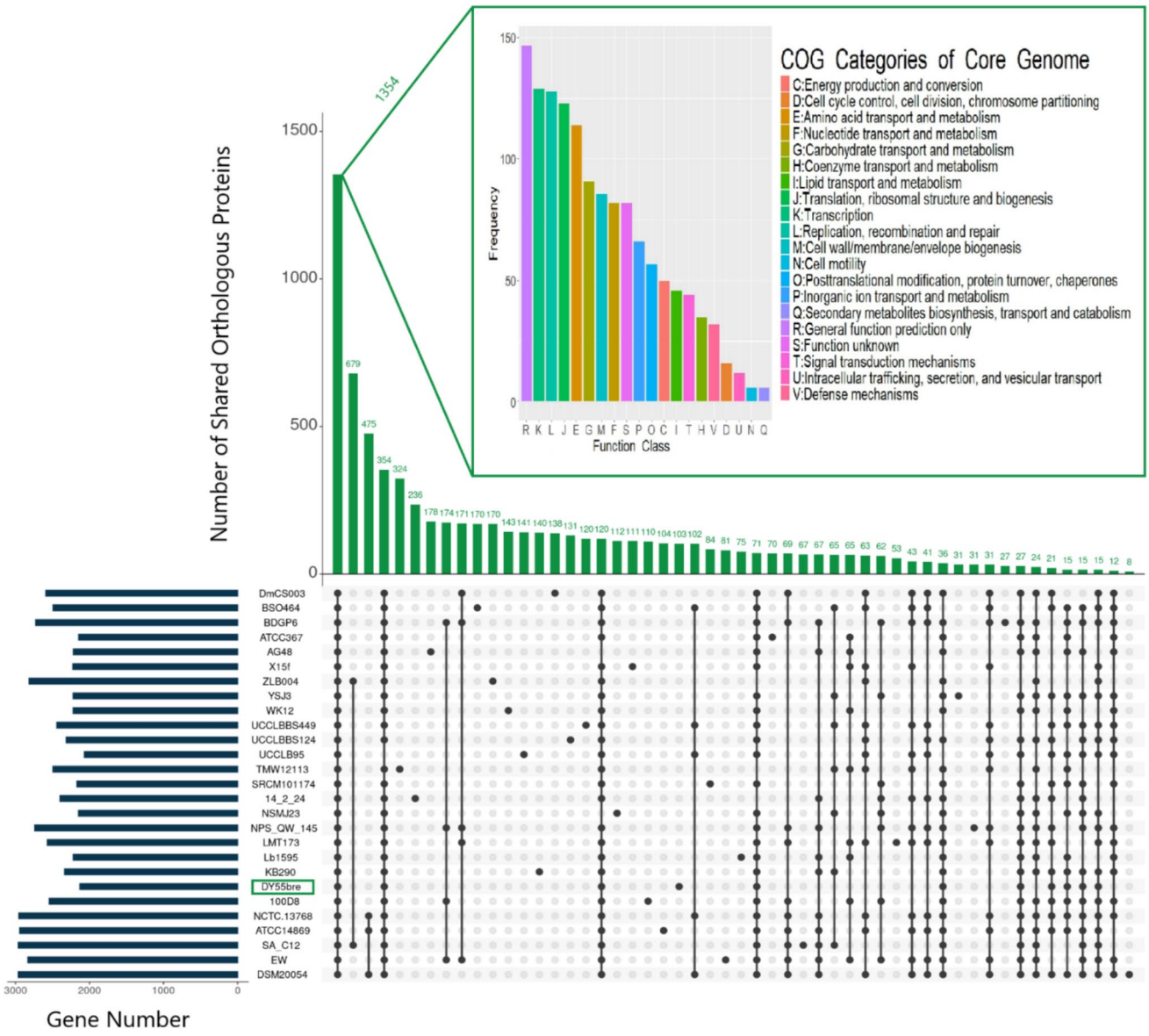

Fig. 4 The Upset plot illustrates the quantity of core genome, strain-specific (singletons), and other genes that are considered dispensable. Moreover, it displays clusters of orthologous groups (COGs) associated with the core genome

regulatory protein A]), which are well recognized for their roles in host adhesion, immune modulation, and biofilm formation traits essential for effective probiotic function [71–73]. Additionally, the exclusive presence of metabolic genes such as agmatine deiminase (CLUSTER5447) and carbamate kinase (CLUSTER5997) in DY55bre suggests enhanced acid resistance, nitrogen metabolism, and energy production, which may facilitate survival and persistence in the gastrointestinal tract and during fermentation processes [74, 75]. The identification of genes involved in cell wall biosynthesis and genome maintenance further indicates that DY55bre may possess superior environmental adaptability and genomic stability compared to YSJ3 and SA_C12 [71, 72]. Collectively, these findings underscore the functional distinctiveness of DY55bre and support its potential as a strong probiotic candidate.

In Vitro and In Silico Safety Assessment

The antibiotic susceptibility of strain DY55bre was assessed in line with the performance standards defined by the Clinical and Laboratory Standards Institute. The DY55bre strain was tested against 14 different antibiotics, and their zone of inhibition (ZOI) values are displayed in Table 1. The strain DY55bre exhibited resistance (ZOI ≤ 14 mm) to ampicillin (10 µg/disc), methicillin (5 µg/disc), oxacillin (1 µg/disc),

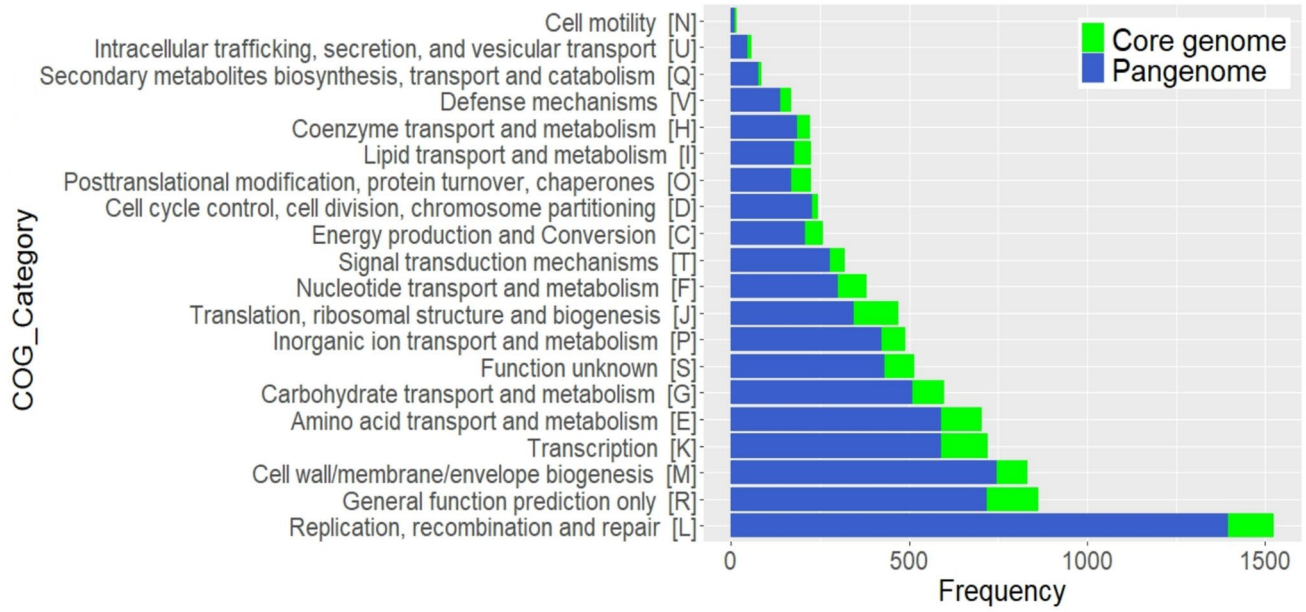

Fig. 5 The number of COG categories observed in the core (green) and pangenome (blue) of 27 genomes of *Lvb. brevis*

streptomycin (10 µg/disc), amikacin (30 µg/disc), kanamycin (30 µg/disc), vancomycin (30 µg/disc), and tetracycline (30 µg/disc). Additionally, DY55bre showed sensitivity (ZOI ≥ 20 mm) to carbenicillin (100 µg/disc), amoxycillin (25 µg/disc), azithromycin (15 µg/disc), erythromycin (10 µg/disc), and rifampacin (5 µg/disc), except for penicillin G (10 U/disc). As well, it exhibited moderate susceptibility (15 ≤ ZOI ≤ 19 mm) exclusively to penicillin G (Table 1).

We conducted resistome screening using the BV-BRC and KEGG databases. According to the CARD database, no antibiotic-resistance genes were detected in the genome of DY55bre. However, we identified 46 genes associated with antibiotic resistance using the KEGG and BV-BRC databases. The observed genes have been connected with drug targets (16), vancomycin (6), beta-lactams (9), nitroimidazole (1), streptomycin (1), macrolides and lincosamides (1), triclosan (1), cationic antimicrobial peptides (7), antibiotics that modify cell wall charge (2), and multidrug efflux pumps (1). At first glance, antibiotic target genes and their drugs have garnered significant interest and can be sorted as follows: *Alr* (D-cycloserine), *Ddl* (D-cycloserine), *EF-G* (fusidic acid), *EF-Tu* (kirromycin, enacyloxin IIa, pulvomycin), *folA* (trimethoprim, brodimorphim, tetroxoprim, iclaprim), *gyrA* (clofazimine, ciprofloxacin, gatifloxacin, levofloxacin, moxifloxacin, nalidixic acid, ofloxacin, sparfloxacin, trovafloxacin), *gyrB* (clofazimine, gatifloxacin, ciprofloxacin, levofloxacin, moxifloxacin, nalidixic acid, ofloxacin, sparfloxacin, novobiocin, coumermycin A1, clorobiocin, coumermycin, trovafloxacin), *Iso-tRNA* (mupirocin), *inhA* (isoniazid, ethionamide, triclosan), *kasA* (isoniazid, triclosan), *MurA* (fosfomycin), *rpoB* (rifamycin, daptomycin, rifabutin, rifampin), *rpoC* (daptomycin), *S10p* (tetracycline, tigecycline), and *S12p* (streptomycin).

Likewise, the vancomycin-related resistance genes were identified as *vanX*, *murG*, *murF*, *mraY*, *ddl*, and *alr*, based on the KEGG annotation results. *Lactobacillus* species are widely recognized for their resistance to vancomycin due to intrinsic peptidoglycan precursors containing D-lactate instead of D-alanine at the C-terminus. In addition, the *VanX* gene exhibits a high specificity in its ability to hydrolyze D-alanine-D-alanine dipeptides. This gene also plays a vital role in forming cell walls. In addition, the *gidB* gene, responsible for streptomycin resistance, has been identified. It generates the enzyme 7-methylguanosine methyltransferase, which specifically targets the 16S rRNA. Genetic mutations in this specific gene were reported to be the source of resistance to streptomycin and other aminoglycosides [76–78]. A nitroimidazole class antibiotic resistance gene of *NimB* has been identified, which is responsible for synthesizing the nitroimidazole reductase enzyme. This enzyme deactivates antibiotics of the nitroimidazole group, such as metronidazole [79]. The *RlmA*(II) gene has been identified to resist mycinamicin, tylosin, and lincosamides. It was reported that this resistance is caused by the methylation of the N1-position of nucleotide G748 in the 23S rRNA [80]. Further, a bacterial 3-oxoacyl enoyl-acyl carrier reductase enzyme encoding the *fabV* gene has been detected, which confers resistance to the biocide triclosan [81].

Meanwhile, the existence of the *ykkCD* gene, which encodes a multidrug efflux pump, has been verified,

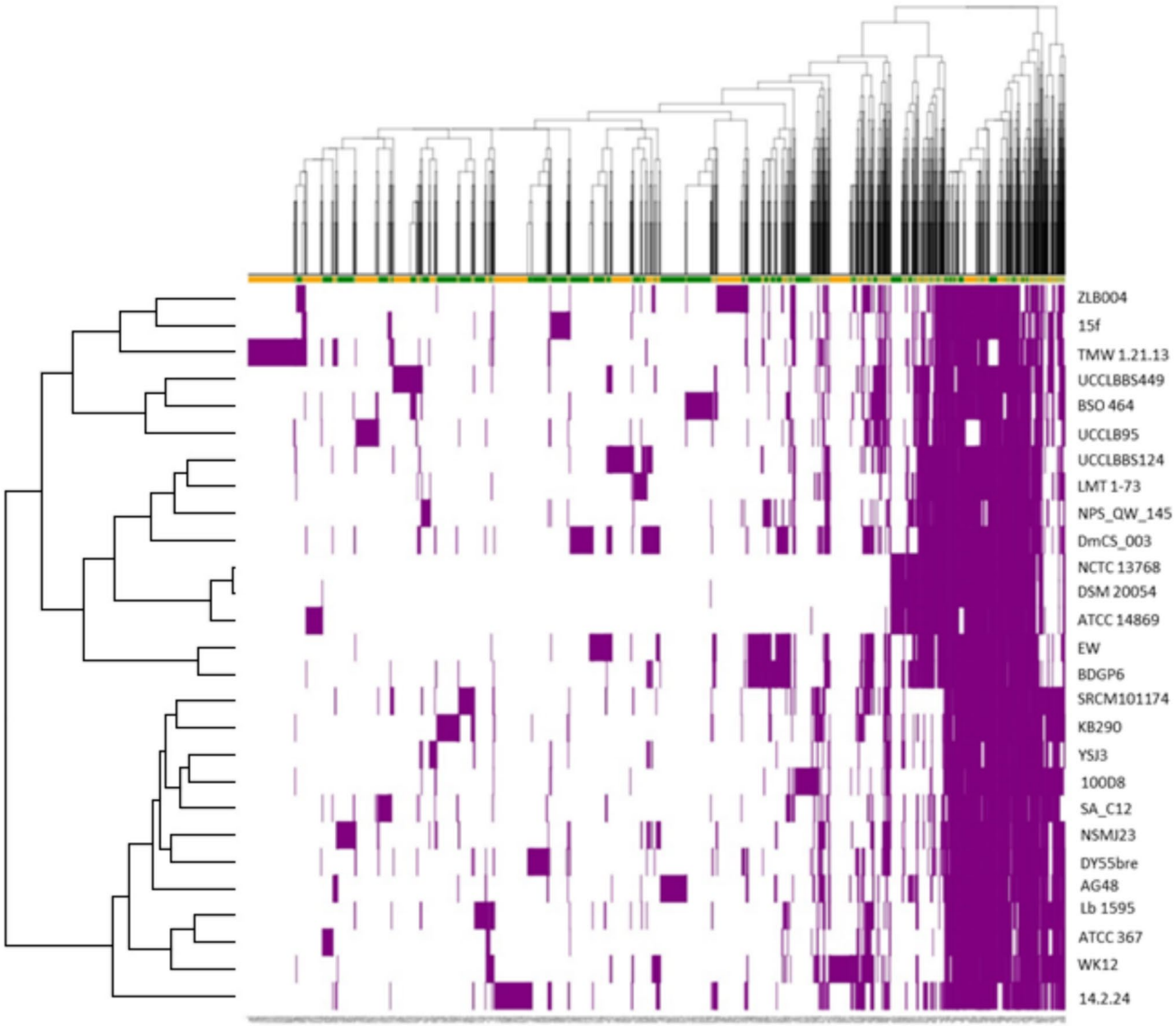

Fig. 6 Matrix showing the presence or absence of clusterized accessory genes. Genes are colored if they are found in the genome. Gene clusters and genomes have been arranged by hierarchical clustering

including two subunits of SMR (small multidrug resistance) type proteins. It exhibits resistance to cationic medicines, namely chloramphenicol, streptomycin, and tetracycline [82]. The existence of cell wall charge-altering protein encoding *GdpD*, *MprF*, and *PgsA* genes, which provide antibiotic resistance against daptomycin and defensin, has been verified via BV-BRC [83, 84]. Notably, we have detected the presence of genes encoding elements of the oligopeptide transport system associated with beta-Lactam resistance (*oppA*, *oppB*, *oppC*, *oppD*, *oppF*, and *AbcA*), as well as genes expressing penicillin-binding protein 1 A (*mrcA*) and 2 A (*pbp2A*), and beta-lactamase class A (*PenP*). Recently, various researchers have reported the occurrence of penicillin G resistance and confirmed the availability of the previously mentioned resistome associated with beta-lactams in certain strains of *Lactiplantibacillus plantarum*, *Limosilactobacillus reuteri*, and *Lacticaseibacillus rhamnosus* [18, 85, 86]. These data further corroborate the results of the present study. The existence of transferable antimicrobial resistance genes in probiotics, which are used for humans or animals, is undesirable due to concerns about different food niches and common bacteria that could potentially serve as reservoirs for the resistome. Lactobacilli possess inherent resistance to many antimicrobial substances, and it is widely recognized that this resistance is not associated with specific safety issues. However, the intrinsic resistome on the bacterial chromosome must not be flanked by transposases or integrases. The protein BLAST analysis did not identify

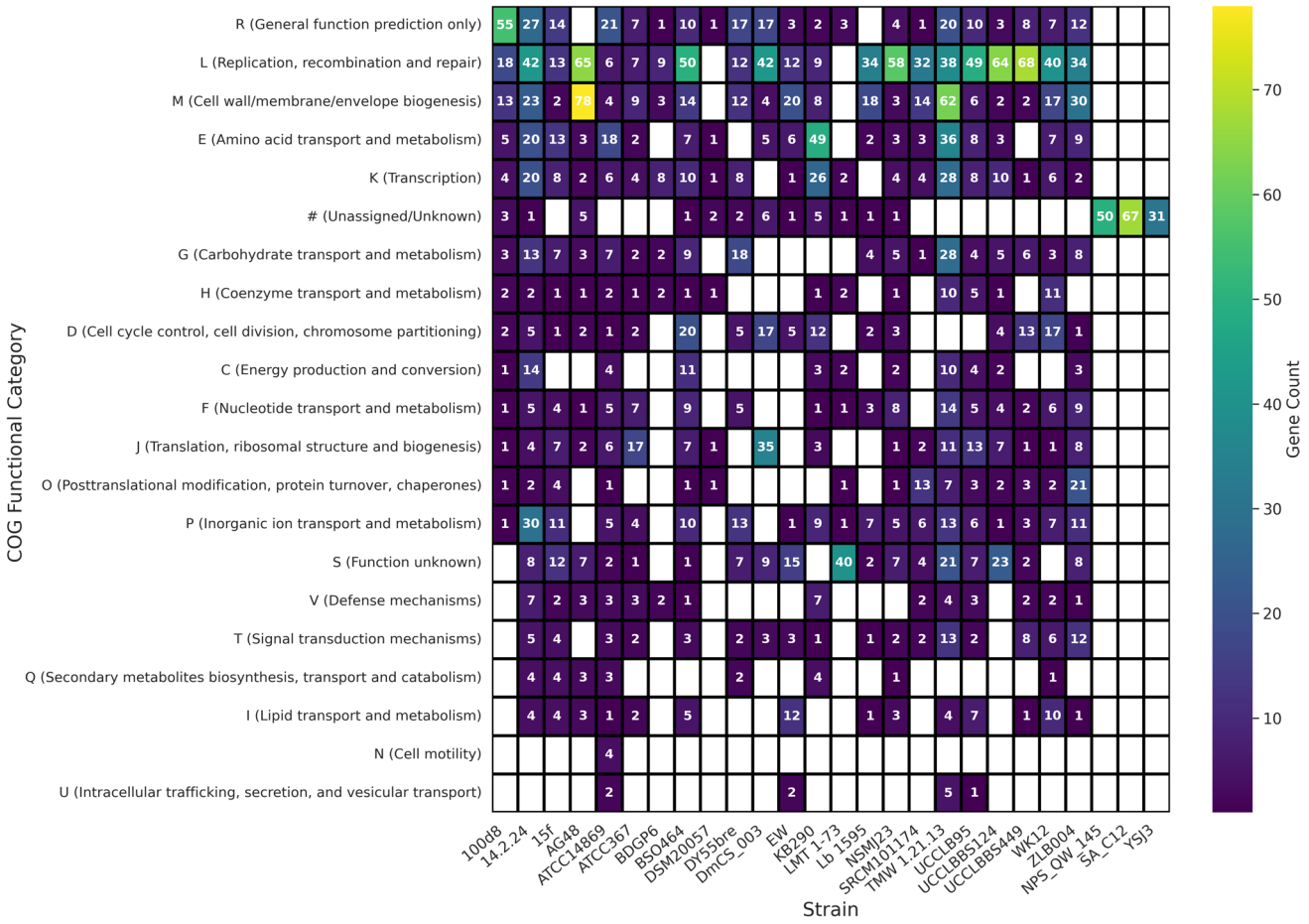

Fig. 7 Distribution of COG functional categories for strain-specific genes (singletons) identified in the analyzed *Lvb. brevis* genomes. White blocks in the heatmap mean that no genes were found related to the respective COG functional category

any horizontally transferred genes in the target resistome (Table S9). Additionally, the pDY55bre plasmid (CP136802) has no antibiotic-resistance genes. These findings align with EFSA guidelines, indicating that intrinsic resistance in lactobacilli does not pose a safety concern for probiotic usages [87, 88].

Carbohydrate Fermentation Patterns and CAZYmes

Lvb. brevis obtains ATP via engaging in heterofermentative carbohydrate fermentation, which depends on the strain's affinity for sugars [2]. Identifying strain-specific metabolic characteristics is crucial for predicting their potential industrial application and probiotic benefits. *Lvb. brevis* has an adaptive nature and can ferment a variety of carbohydrates. The API 50 CHL carbohydrate fermentation test revealed that DY55bre can metabolize a total of 13 sugars, including L-arabinose, D-ribose, D-xylose, D-galactose, D-glucose, N-acetylglucosamine, esculin ferric citrate, D-maltose, D-melibiose, D-sucrose, and D-melezitose. The strain's ability to utilize carbohydrates directly depends on the presence of genes responsible for transporters and CAZYmes [89].

Most transporters involved in carbohydrate metabolism are located inside the phosphoenolpyruvate-dependent sugar phosphotransferase system (PTS) [90]. The genome of strain DY55bre possesses the majority of phosphotransferase system (PTS) enzymes. This includes the PTS enzyme I (*ptsI*), the gene for the phosphocarrier protein HPr (*ptsH*, also known as a proton carrier), the gene for the fructose transporter-specific multiphosphoryl transfer protein (*fruB*, also known as a proton carrier), and the gene for fructose PTS system (*fruA*) and other substrate-specific transporter complexes, which are summarized in Table S7. In addition, carbohydrate-specific ABC transporters are given in the same table. The KEGG annotation results suggest that the remaining carrier complexes are selective for various carbohydrates and sugar molecules, including maltose, maltodextrin, glucose, mannose, galactose oligomers, maltooligosaccharides, arabinooligosaccharides, raffinose, stachyose, melibiose, sorbitol, mannitol, alpha-glucoside, cellobiose,

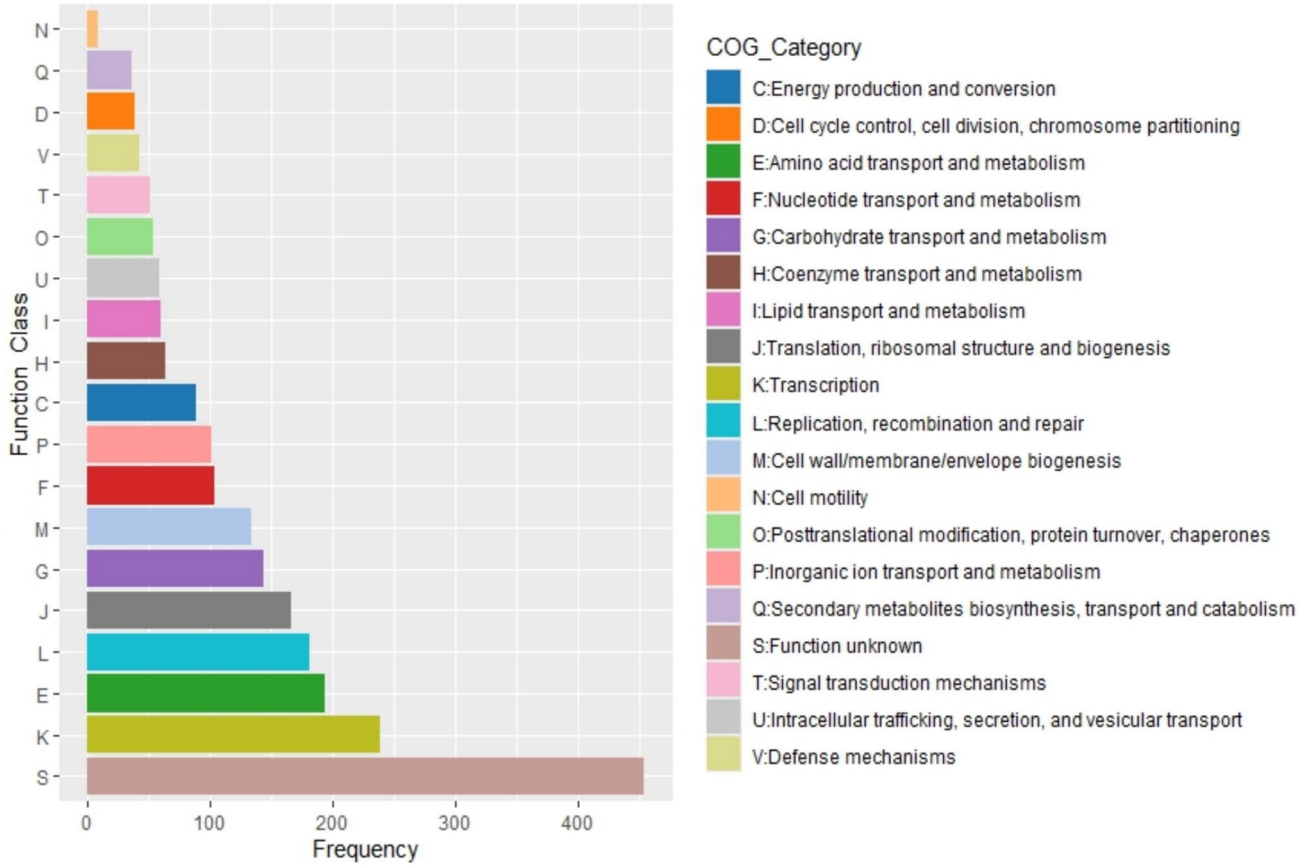

Fig. 8 Visual representation of the identified numbers of clusters of orthologous groups (COG) of protein-coding sequences in the genome of *Lvb. brevis* DY55bre using eggNOG mapper

Table 1 Antibiotic susceptibility test results of *Lvb. brevis* strain DY55bre

Antibiotic group	Antibiotic	Zone diameter/status*
β-Lactams	Ampicillin (10 µg/disc)	≤ 14 ± 0.2 mm (R)
	Methicillin (5 µg/disc)	Not detected (R)
	Oxacillin (1 µg/disc)	Not detected (R)
	Penicillin G (10 U/disc)	14.7 ± 0.35 mm (I)
	Carbenicillin (100 µg/disc)	21.1 ± 0.6 mm (S)
	Amoxycillin (25 µg/disc)	24 ± 0.16 mm (S)
Aminoglucosides	Streptomycin (10 µg/disc)	Not detected (R)
	Amikacin (30 µg/disc)	≤ 14 ± 0.13 mm (R)
	Kanamycin (30 µg/disc)	Not detected (R)
Vancomycin	Vancomycin (30 µg/disc)	Not detected (R)
Macrolides	Azithromycin (15 µg/disc)	20.6 ± 0.04 mm (S)
	Erythromycin (10 µg/disc)	24.1 ± 0.3 mm (S)
Tetracyclines	Tetracycline (30 µg/disc)	≤ 14 ± 0.5 mm (R)
Rifamycins	Rifampacin (5 µg/disc)	27.2 ± 0.8 mm (S)

**R* resistant, *I* intermediate/semi-sensitive, *S* sensitive

chitobiose, ribose, D-xylose, diacylchitobiose, and L-ascorbate. Nevertheless, it is well recognized that several sugar transporters can import more than one substrate [91].

Heterofermentative species have been frequently equipped with the *araBAD* operon, which includes L-ribulokinase (*araB*), L-arabinose isomerase (*araA*), and L-ribulose-5P-4-epimerase (*araD*), and has been associated with the breakdown of L-arabinose, a critical step in heterofermentation [2]. Similarly, the *araBAD* operon has been found in the DY55bre genome. Additionally, the DY55bre genome misses 1-phosphofructokinase (*pfK*) and fructose-1,6-bisphosphate aldolase enzymes; hence, it is unable to use hexoses via the EMP pathway due to the absence of the aforementioned enzymes. Instead, it breaks down the hexoses via the phosphogluconate pathway (Fig. 9), producing not only lactic acid but also considerable amounts of ethanol, acetate, and CO_2 [16, 92]. This finding confirmed that DY55bre has an obligatory heterofermentative metabolism. Moreover, transketolase (*tktA*), phosphoketolase (*xpf*), and glucose-6P-isomerase (*pgi*) genes have also existed in its genome, as previously reported for *L. fermentum* [13]. The presence of the enzymes involved in the degradation of sucrose, maltose,

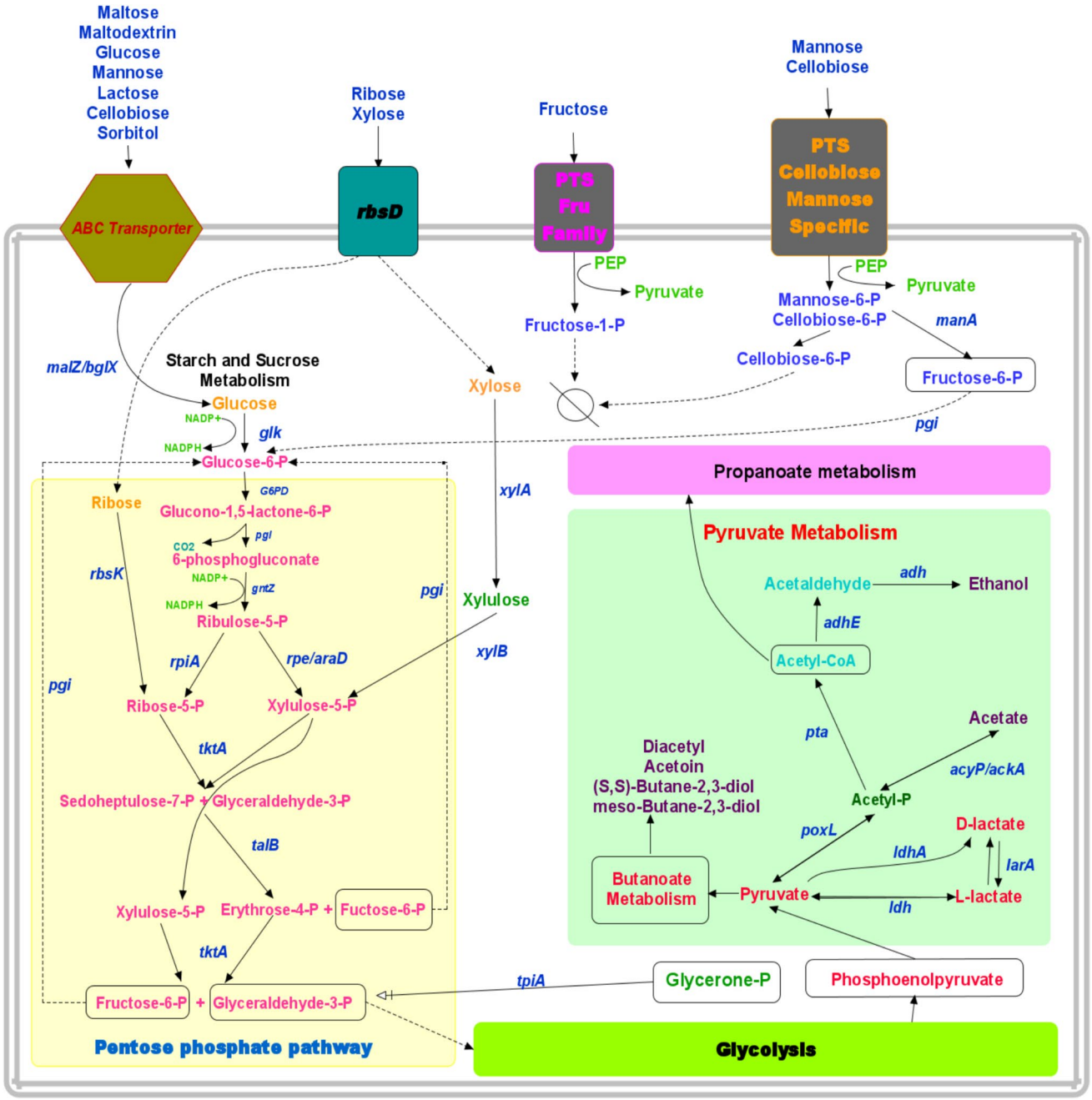

Fig. 9 Summary of the putative carbohydrate metabolism of *Lvb. brevis* DY55bre strain based on KEGG pathway modules. The exact names of the associated genes are as follows: *rbsD*; D-ribose pyranase [EC:5.4.99.62]; *manA*; mannose-6-phosphate isomerase [EC:5.3.1.8]; *pgi*, glucose-6-phosphate isomerase [EC:5.3.1.9]; *glk*, glucokinase [EC:2.7.1.2]; *malZ,* alpha-glucosidase [EC:3.2.1.20]; *bglX*, beta-glucosidase [EC:3.2.1.21]; *glk*, glucokinase [EC:2.7.1.2]; *G6PD*, glucose-6-phosphate 1-dehydrogenase [EC:1.1.1.49; 1.1.1.363]; *pgl*, 6-phosphogluconolactonase [EC:3.1.1.31]; *gntZ*, 6-phosphogluconate dehydrogenase [EC:1.1.1.44; 1.1.1.343]; *rbsK*, ribokinase [EC:2.7.1.15]; *rpiA*, ribose 5-phosphate isomerase A [EC:5.3.1.6]; *rpe*, ribulose-phosphate 3-epimerase [EC:5.1.3.1]; *araD*, L-ribulose-5-phosphate 4-epimerase [EC:5.1.3.4]; *tktA*, transketolase [EC:2.2.1.1]; *talB*, transaldolase [EC:2.2.1.2]; *tpiA*, transaldolase [EC:2.2.1.2]; *ldh*, L-lactate dehydrogenase [EC:1.1.1.27]; *larA*, lactate racemase [EC:5.1.2.1]; *ldhA*, D-lactate dehydrogenase [EC:1.1.1.28]; *poxL*, pyruvate oxidase [EC:1.2.3.3]; *pta*, phosphate acetyltransferase [EC:2.3.1.8]; *adhE*, acetaldehyde dehydrogenase [EC:1.2.1.10]; *adh*, alcohol dehydrogenase [EC:1.1.1.1]

and glucose, namely alpha-glucosidase, sucrose alpha-glucohydrolase, and beta-glucosidase, was also verified. Even though DY55bre is a plant-derived *Lvb. brevis* strain, the presence of *lacZ*, *galE*, *galM*, *galK*, *galU*, *lacA*, *galT*, *malZ*, *pgm*, *glf*, *galA*, and *glk* genes of galactose metabolism was observed in its genome (Table S8). This might be attributed to the free-living and obligatory heterofermentative lifestyle of *Lvb. brevis* [2, 55]. The identification of xylose isomerase (*xylA*) and xylulokinase (*xylB*) genes, responsible for catalyzing the conversion of xylose into xylulose-5P before entering glycolysis as glyceraldehyde-3P, was also fulfilled.

DY55bre comprises 24 distinct genes encoding pyruvate metabolism enzymes, some of which have multiple copies, such as alcohol dehydrogenase (*adh*; 2) and acetate kinase (*ackA*; 3). At first glance, the presence of pyruvate kinase (*pyk*), an enzyme responsible for converting phosphoenolpyruvate to pyruvate, also attracted notice. The availability of L-lactate dehydrogenase (*ldh*) and D-lactate dehydrogenase (*ldhA*) genes indicated the capability of DY55bre to produce D- and L-isomers of lactic acid from pyruvate. In addition, it contains lactate racemase (*larA*), an enzyme responsible for the reversible conversion of D- and L-enantiomers of lactate. The malolactic enzyme, which is also part of pyruvate metabolism, catalyzes the conversion of malate into lactate and CO_2. Apart from that, the existence of two copies of alcohol dehydrogenase (*adh*) and two copies of propanol-preferring alcohol dehydrogenase (*adhP*) on the DY55bre genome is noteworthy. The *adh* gene catalyzes the conversion of acetaldehyde into ethanol, while *adhP* can reversibly produce aldehydes from primary alcohols [93]. During the conversion of pyruvate to ethanol, pyruvate is first transformed into acetyl-CoA by the pyruvate dehydrogenase complex. Subsequently, acetyl-CoA is turned into acetaldehyde, which is further converted into ethanol by the enzymes acetaldehyde dehydrogenase (*adhE*) and alcohol dehydrogenase (*adh*), respectively. As an alternative pathway, pyruvate can also be converted into acetyl phosphate and then acetate by the action of pyruvate oxidase (*poxL*) and acetate kinase (*ackA*), respectively, to synthesize ATP.

Following glycolysis, pyruvate is transformed to (S)−2-acetolactate and subsequently to diacetyl and acetoin by the enzymes acetolactate synthase (*ilvB*), acetolactate decarboxylase (*alsD*), and diacetyl reductase (*budC*) [94]. Subsequently, both enantiomers of (S)−2-acetoin and (R)−2-acetoin may be transformed into (S, S)-butane-2,3-diol or (R, R)-butane-2,3-diol, respectively, by butanediol dehydrogenase (*butA*) [95]. Except for those, it has been revealed that there is a deficiency in the members of the *pdu* operon, responsible for the metabolic conversion of glycerol into 1,2-propanediol, pronanal, 1-propanol, or propanoate. The enzymes converting glycerol to glycerone-P and then to methylglyoxal were not detected. But, enzymes like glycerol dehydrogenase and B12-dependent propanediol dehydratase (*pduCDE*) are available; the former converts hydroxyacetone to 1,2-propanediol, and the latter transforms 1,2-propanediol to propanal [96]. Surprisingly, the *cbi* operon (cobalamin, B12-biosynthesis), crucial for *pduCDE* functioning, was absent from the DY55bre genome. Conversely, in exogenous cobalamin, the strain can synthesize 1-propanol from propanol via 1-propanol dehydrogenase (*pduQ*) [97, 98].

As determined by KEGG mapper reports, the DY55bre genome encodes 190 carbohydrate metabolism-related genes. These genes are distributed as follows: 14 starch and sucrose metabolism genes, 9 fructose and mannose metabolism genes, 12 galactose metabolism genes, 19 pentose phosphate pathway genes, 17 pentose and glucuronate interconversion-associated genes, 19 glycolysis-related genes, 24 amino sugar and nucleotide sugar metabolism genes, 7 ascorbate and aldarate metabolism genes, 24 pyruvate metabolism genes, 5 TCA cycle-related genes, 10 glyoxylate and dicarboxylate metabolism genes, 16 propanoate metabolism genes, 10 butanoate metabolism genes, 2 inositol phosphate metabolism genes, and 2 C5-branched dibasic acid metabolism genes. Furthermore, 47 glycoside hydrolases, 37 glycosyltransferases, 12 carbohydrate-binding modules, 1 auxiliary activity, and 2 carbohydrate esterases encoded in the DY55bre genome were found as a result of dbCAN3 analysis [37]. In summary, evaluation results revealed that DY55bre not only has the potential to produce industrially crucial plate-form chemicals Like lactic acid, acetic acid, ethanol, 1-propanol, propanal, and 2,3-butanediol but also some food-grade aroma compounds such as acetaldehyde, acetoin, and diacetyl as an outcome of carbohydrate metabolism.

Prediction of Secondary Metabolites and Associated Gene Clusters of Interest

Bacteria are a significant reservoir of biologically active compounds, such as secondary metabolites [99, 100]. In the DY55bre genome, the T3PKS (beginning at 36.464 end 77.633, total 41.170 nt) and lanthipeptide-class-iv (beginning at 522.503 end 544.950, total 22.448 nt) biosynthetic gene clusters were predicted using the antiSMASH platform. A summary of the T3PKS gene cluster and its ClusterBLAST results is depicted in Fig. S2. A full list of the T3PKS gene cluster's members and their protein-BLAST results is also listed in Table S3. The MIBiG comparison results indicated that the T3PKS gene cluster showed 56% similarity with the viguiepinol cluster, a polyketide derived from *Streptomyces* sp. KO-3988. Moreover, ClusterBLAST output showed 100% similarity with *Levilactobacillus brevis* YSJ3 (CP092264), SRCM101174 (CP021479), DRD-35 (NZ_JAMRWQ010000001), MB13 (NZ_JAJEUF010000002), 100D8 (CP015338), SC013 (CP113250), SMB091

(CP113117), TMW1.2108 (CP019734), ZLB004 (CP021456), and 3M004 (NZ_NFZZ01000001). Hydroxymethylglutaryl-CoA synthase was identified as the primary biosynthetic gene in the T3PKS biosynthetic cluster. This enzyme facilitates the combination of acetyl-CoA with acetoacetyl-CoA to form HMG-CoA and CoA. This reaction is the second step in the biosynthesis pathway of isoprenoids that relies on mevalonate [101]. Besides, the gene cluster showed 52% similarity with phenazine derivatives (SA, SB, and SC) biosynthesis-responsible gene clusters from *Streptomyces*. Clusters of lanthipeptide-class-iv genes were devoid of some cluster components, such as transporters. The core biosynthetic gene of this cluster was identified as lanthipeptide-class-iv: Pkinase by antiSMASH. Conversely, the protein BLAST result revealed that this core gene has been identified as the Lanthionine synthetase *LanC* family protein (WP_139560164.1). Normally, class IV lantipeptides are synthesized by a trifunctional enzyme *LanL*, and class I lanthipeptides are produced by *LanB* (dehydratase) and *LanC* (cyclase) [102].

On the other hand, ClusterBLAST analysis revealed that the lanthipeptide gene cluster exhibited similarity percentages of 57%, 55%, and 52% (last three) with SA-C12 (CP031185), ATCC 367 (NC_008497), NSMJ23 (CP050541), UCCLB556 (CP031174), and UCCLB524 (CP031208), respectively (Fig. S3 and Table S4). It is possible to speculate that the second lanthipeptide gene cluster might be flanked by transposons or a novel gene cluster to be found in *Lvb. brevis* strain DY55bre. Previous studies suggested bacterial secondary metabolites (T3PKSs, RiPPs, or other polyketides) could be associated with apoptosis induction in cancer cells and antimicrobial activity against pathogens [99, 103]. However, no polyketide-structured molecule is detected due to GC-MS analysis. For this study, apoptosis-induced lobule formation in deformed HT29 and DLD-1 cells (Fig. 9G and F) can be associated with cyclic dipeptides and 1,4-diaza-2,5-dioxo-3-isobutyl bicyclo[4.3.0] nonane compound found in the cell-free supernatant of DY55bre.

General Probiotic Characteristics

Probiotic characterization tests were conducted to verify the presence or absence of the characteristics necessary for classification as probiotics. Initially, the findings of the β-hemolysis test proved that DY55bre lacks β-hemolytic activity. Moreover, DY55bre demonstrated 59.3%, 87%, and 60.8% adhesion capacities to HT29, Caco-2, and DLD-1 colorectal adenocarcinoma cell lines, respectively (Table 2). Caco-2 and HT29 cell lines reflect the morphological and biochemical characteristics of the small intestine, while DLD-1 reflects the morphological and biochemical characteristics of the large intestine [104]. Differences in the adhesion capacity (Fig. 10) can be explained

Table 2 Probiotic evaluation test results for *Lvb. brevis* strain DY55bre

Characterization test		Result
β-Hemolysis on Blood Agar		Non-hemolytic
Auto-aggregation (%)		84,55 ± 0,24
Cell-surface hydrophobicity (%)		56,69 ± 0,05
Cholesterol assimilation (%)		27,28 ± 0,82
Antioxidant activity against DPPH (inhibition %)		34,25 ± 0,39
Antioxidant activity against $ABTS^+$ (inhibition %)		76,63 ± 0,42
Adhesion behavior in HT29, Caco-2 and DLD-1 cell lines		
Cell line	**Recovery (%)***	**Adhesion ability (%)**
HT29	40,7	59,3 ± 0,06
Caco-2	13	87 ± 0,01
DLD-1	39,2	60,8 ± 0,15
Antimicrobial activity of cell-free supernatants against test pathogens**		
Test strain		**ZOI (mm)*****
Escherichia coli ATCC 25922		27,42 ± 0,64
Escherichia coli O157:H7 ATCC 43897		16,55 ± 0,28
Bacillus cereus ATCC 33019		20,8 ± 0,30
Salmonella enterica sv. typhimurium ATCC 14028		16,47 ± 0,27
Proteus mirabilis ATCC 29906		16,16 ± 0,87
Enterobacter cloacae ATCC 13047		13,6 ± 0,2

*Recovery (%) was calculated based on the results of adhesion ability (%)

**Cell-free supernatants were concentrated 8 × by freeze-drying only for antibiogram assay

***Zone of inhibition

by the cell wall surface layer protein-network specificity of the DY55bre strain, which showed more affinity to Caco-2 cells than HT29 and DLD-1 cell lines [45]. This protein network is also linked with auto-aggregation capacity and cell surface hydrophobicity; its relationship with encoding genes will be explained in the following paragraphs.

The auto-aggregation capacity (AC) and cell surface hydrophobicity (CSH) were detected to be 84,552 ± 0,249% and 56,697 ± 0.05% (with xylene), respectively (Table 2). The auto-aggregation capacity of probiotic bacteria is critical because of its close association with the adhesion of epithelial cells and mucosal surfaces. Because of the AC, bacteria can form cellular aggregates that enhance their ability

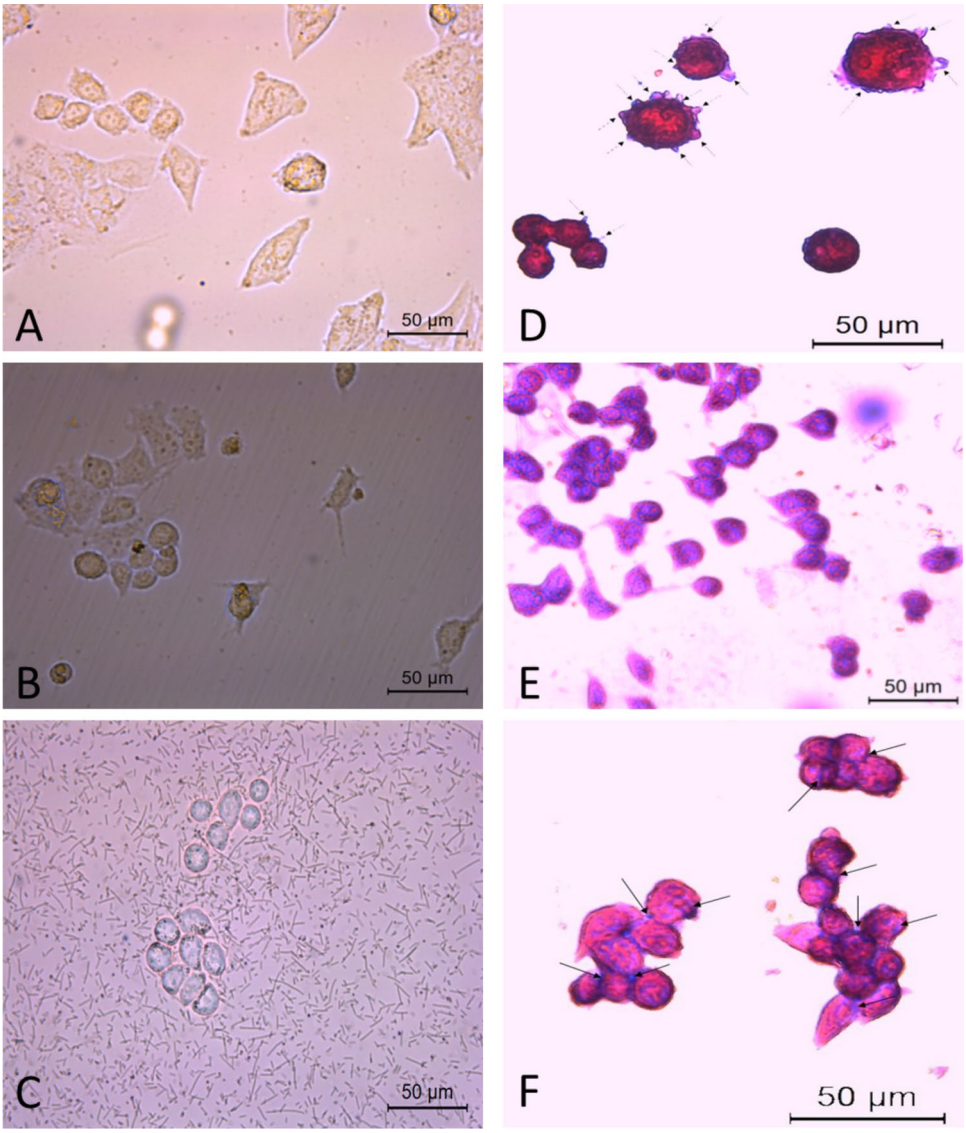

Fig. 10 Microscope images of non-adhered and adhered Lvb. Brevis DY55bre cells to HT29, Caco-2, and DLD-1 colorectal adenocarcinoma cell Lines at × 40 magnification (Leica inverted cell-culture microscope, DM-IL LED, Germany). **A** Growing and cell-culture plate adhered HT29 cells. **B** Growing and cell-culture plate adhered Caco2 cells. **C** Co-cultured DY55bre and DLD-1 cells. **D** DY55bre attached to HT29 cells as indicated by arrows. **E** DY55bre bound to Caco2 cells, which purple spots had identified. **F** The DY55bre cells were adhered to the DLD-1 cell clusters, as illustrated by arrows (purple spots) **G** On the HT29 cell, a green arrow marks lobe formation, an apoptosis induction indicator, while black arrows indicate adhered DY55bre cells. **H** Another image of DY55bre-adhered Caco2 cells that were marked with black arrows. **I** DY55bre cells adhered to DLD-1 cell aggregate; adhered cells are also marked with black arrows. **J** Green arrows indicate apoptosis-induced lobule formation in deformed DLD-1 cells, while black arrows indicate adherent and self-aggregated DY55bre cells. **K** Gram-stained overnight-grown Lvb. brevis cells on MRS broth. The image was captured with a × 100 objective of light microscope (Leica DM500, Germany), and additionally, 3.2 × Xiaomi Redmi 9 T digital AI zoom has been applied

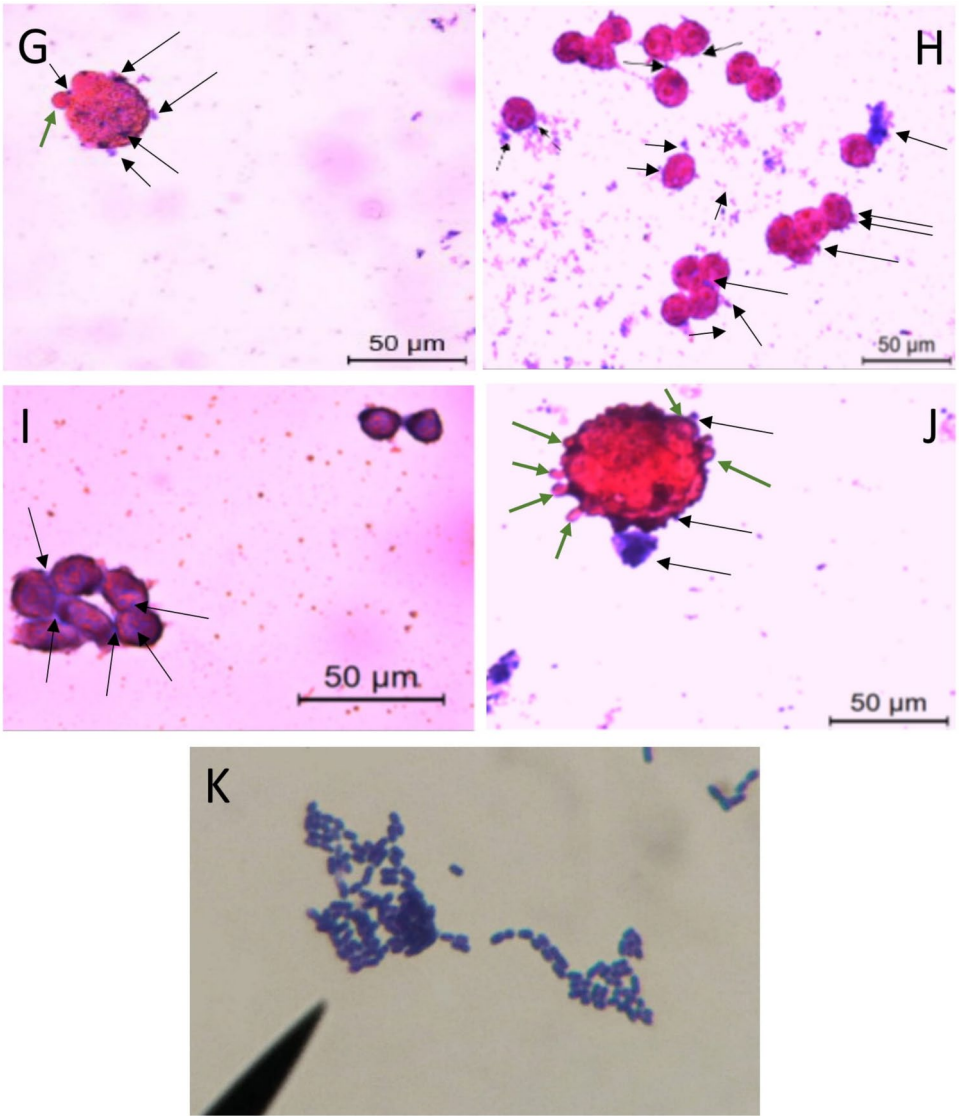

Fig. 10 (continued)

to remain in the colon (Fig. 10H and F). Bacterial cell wall components, together with mucus-binding proteins, adhesins, surface layer proteins, fibronectin-binding proteins, exopolysaccharides, and lipoteichoic acids, confer a distinct advantage to bacteria in terms of their ability to colonize and adhere to host epithelial cells [13]. DY55bre genome includes 19 genes encoding adhesion-related putative proteins such as maltose phosphorylase (*mapA*), lipoprotein-anchoring transpeptidase (*efrK/sfrK*), elongation factor Tu (*ef-tu*), triosephosphate isomerase (*tpiA*), glyceraldehyde 3-phosphate dehydrogenase (*gapA*), β-galactosidase (*lacZ*), LPXTG specific sortase A (*srtA*), isopeptide-forming pilin-related protein (*spaA*), LPXTG specific collagen adhesin (*lmo0159*), putative peptidoglycan bound protein (*lmo0160*), LPXTG motif-containing internalin-like proteins (*lmo0732* and *lmo2396* homologs), tyrosine-protein kinase (*epsD*), tyrosine-protein kinase transmembrane modulator (*epsC*), UDP-N-acetylglucosamine-N-acetylmuramyl-(pentapeptide) pyrophosphorylase-undecaprenol N-acetylglucosamine transferase (*murG*), and enolase. Previous studies reported that most of these genes are adhesion-related [13, 89, 105]. Notably, the type and copy number of internalin-like proteins containing the LPXTG motif vary among the strains (Supplemental Excel sheet for Probiotic traits).

Another critical factor in determining the overall adhesion ability of probiotics is the CSH, which is often evaluated by examining the bacterial affinity to a hydrocarbon solvent such as xylene, n-hexadecane, or hexane. It is reported that bacteria with higher cell surface hydrophobicity may adhere more effectively to intestinal epithelial cells [13, 106]. Additionally, the minimum hydrophobicity value required for a probiotic strain is reported to be

40% by Del Re et al. [107]. Xylene was selected as the apolar solvent in this work because of its dual properties of hydrophobicity and hydrophilicity [108]. In previous studies, different CSH values were reported for *Lvb. brevis* HL6 (48.53%), G1 (~48%), KU15006 (~49%), MW08466 (63.32%), RAMULAB52 (72.25%), and CCMA1284 (95.33%). Depending on the strain, these differences might originate from variations in cell surface lipoteichoic acid types and amounts. Cell wall teichoic acids and their associated substituents are widely recognized for their role in imparting bacterial cell surface charge and hydrophobicity, thereby influencing the binding of external molecules. This function protects bacteria against various dangers and unsuitable situations [109].

In this study, CSH-related genes (*dltA*, *dltB*, *dltC*, *dltD*, *dltX*, *TagG*, *TagH*, *LtaS*, and O-antigen membrane protein) have been identified in the DY55bre and compared with other *Lvb. brevis* genomes in the Supplemental Excel sheet for Probiotic traits. Besides, some of these genes are critical to immunomodulatory (*dltA*, *dltB*, *dltC*, *dltD*, *dltX*). Moreover, the *LuxS* gene is linked to anti-pathogenic effects and quorum sensing. Quorum sensing (QS) is the mechanism by which bacteria establish communication with one another through the release of chemical signals known as autoinducers (AIs). Thus, this mechanism controls bacterial biofilm formation, and the *LuxS* gene is highly conserved and ubiquitous in Gram (+) and Gram (-) bacteria. He et al. [110] found a direct relationship between the *LuxS* gene and cell surface hydrophobicity. In addition to their function in carbohydrate metabolism, the xylose isomerase (*xylA*) and xylokinase (*xylB*) genes are involved in gut persistence [13, 111].

The ability of lactobacilli to withstand gastrointestinal stressors, including prolonged survival and colonization, is distinctive. The elucidation of host–probiotic interaction regulatory mechanisms has gained prominence due to the rising prevalence of microorganisms employed as probiotics [13]. The survival traits of DY55bre were evaluated under physiological pH and bile salt conditions, and the INFOGEST in vitro static gastrointestinal simulation protocol was conducted. The survivability of most lactobacilli at low pH ranges from 2.5 to 3.5, serving as a critical selection criterion for potential acid-tolerant probiotic strains. Probiotics must endure a pH of 3.0 during gastric transit and remain viable for at least 4 h before reaching the lower gastrointestinal tract [112, 113]. The DY55bre exhibited tolerance to acidic conditions, showing a microbial load of 7.82 log CFU/mL at pH 3.0, down from an initial load of 8.82 log CFU/mL at pH 7.0. The viability is reduced to 3.08 log CFU/mL at pH 2.0 (Fig. 11B), particularly aligning with previous study findings [114]. Additionally, the survival pattern to bile salts (0.1–1% (w/v)) was examined, revealing that DY55bre exhibited a notably high survival rate (8.37 log CFU/mL) after 4 h, starting from an initial concentration of 8.69 log CFU/mL (Fig. 11A). It is generally recommended that a bile salt concentration of roughly 0.3% is suitable for probiotic selection [115]. The survival of DY55bre in a simulated gastrointestinal environment was assessed using the INFOGEST approach to determine the strain's tolerance to the competitive conditions of the gastrointestinal tract.

Gastrointestinal tolerance is crucial for probiotics' colonization and metabolic activity to benefit the host [116]. The survival rate was observed to be 8.38 log CFU/mL at the end of the digestion simulation, with an initial load of

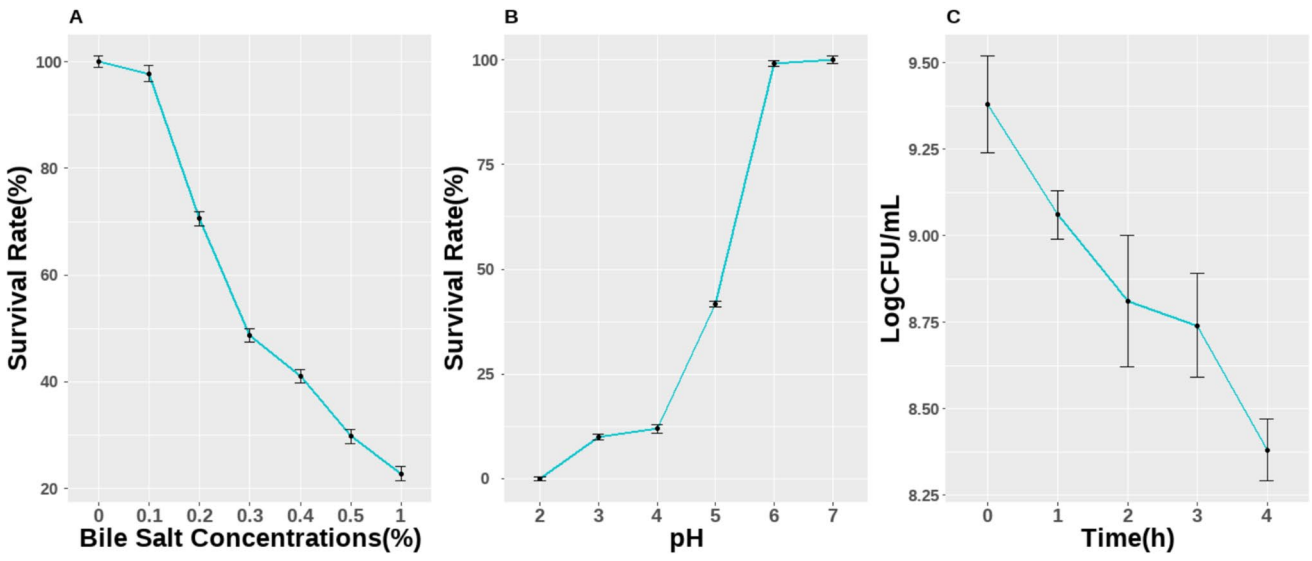

Fig. 11 Growth characteristics and survival rate in various environments of *Lvb. brevis* strain DY55bre. **A** Survival at multiple concentrations of bile salts. **B** Growth at different pH levels. **C** Static in vitro gastric digestion simulation results based on the INFOGEST protocol

9.37 log CFU/mL (Fig. 11C). The resistance to the specified stress factors is linked to the presence of putative genes associated with stress resistance, DNA, and protein protection/repair, as detailed in the Supplemental Excel sheet for Probiotic traits. Cation–proton antiporters (*NhaC*, *gadC*), F-type proton-transporting ATPases, and chaperones (Clp ATPases) play essential roles in maintaining homeostasis and regulating intracellular pH, contributing to acid and bile resistance. Likewise, comparable mechanisms of acid bile resistance were pointed out in different *Lactobacillus* species [13, 17, 18, 116–118]. Moreover, choloylglycine hydrolase (*cbh*, EC 3.5.1.24), inorganic pyrophosphatases (e.g., *PpaC*), and cyclopropane-fatty-acyl-phospholipid synthase (*cfa*, EC 2.1.1.79) are considered significant contributors to bile resistance.

The probiotic genes of *Lvb. brevis* genomes, including DY55bre, were also compared as demonstrated in the Supplemental Excel sheet for Probiotic traits. In brief, the lipoprotein-binding transpeptidase (*ErfK/SrfK*), which facilitates adhesion capacity, was exclusively identified in DY55bre among the analyzed *Lvb. brevis* genomes. Conversely, the *LPXTG lmo0160*, *LPXTG Lmo0732*, and *LPXTG Lmo2396* motifs have been previously identified in DY55bre, while the occurrence of *LPXTG Lmo2178* and *LPXTG Lmo2276* motifs varies among the analyzed *Lvb. brevis* genomes. The D-Ala-teichoic acid biosynthesis protein (*dltX*), which plays a role in immunomodulation, was identified in the DY55bre genome, whereas it was lacking in most of the analyzed *Lvb. brevis* genomes. Moreover, many probiotic genes display variation in copy number across different genomes.

Cytotoxicity and Cyclic Dipeptides

The cytotoxic effects of *Lvb. brevis* DY55bre cell-free supernatants (CFS) were evaluated in HT-29 and DLD-1 colorectal adenocarcinoma cell lines using the CCK-8 assay. As shown in Fig. 11, increasing concentrations of CFS resulted in a dose-dependent reduction in cell viability in both cell lines. For HT-29 cells (Fig. 12A and B), treatment with CFS significantly decreased cell viability compared to the untreated control (0 mg/mL CFS). The IC50 value for HT-29 cells was 7.71 mg/mL, indicating a moderate sensitivity to the supernatant. In contrast, DLD-1 cells (Fig. 12C and D) exhibited a greater sensitivity to CFS treatment, with a lower IC50 value of 3.19 mg/mL, suggesting a stronger anti-proliferative effect in this cell line. These findings highlight the potential of *Lvb. brevis* DY55bre-derived bioactive compounds in inhibiting colorectal cancer cell proliferation. The differential sensitivity between HT-29 and DLD-1 cells suggests that specific molecular mechanisms may influence the cytotoxic effects of CFS, warranting further investigation

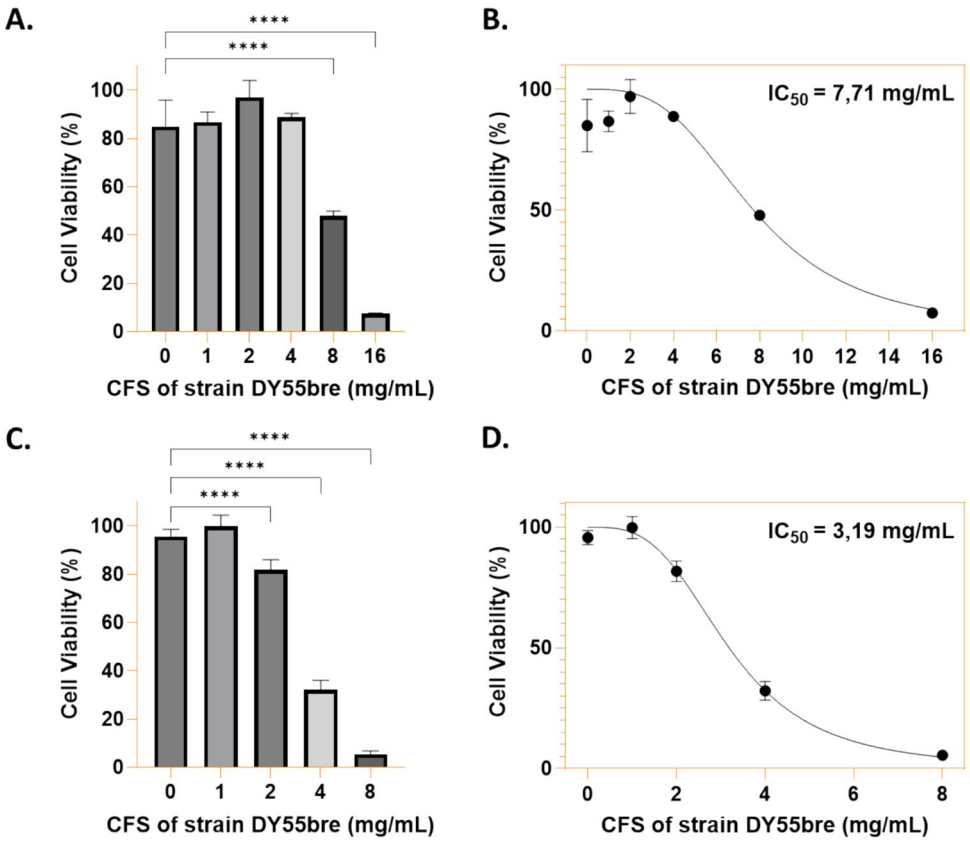

Fig. 12 Results of the CCK-8 assay were obtained by analyzing the cell-free supernatants (CFS) of *Lvb. brevis* DY55bre on the HT29 (**A**, **B**) and DLD-1 (**C**, **D**) colorectal adenocarcinoma cell Lines; 0 mg/mL CFS means the sample without CFS.

into the active components and pathways involved. However, previous studies on diketopiperazines, which are also known as cyclic dipeptides, revealed that cyclo(L-Leu-L-Pro), cyclo(L-Phe-L-Hyp), cyclo(L-Phe-D-Pro), cyclo(D-Phe-D-Pro), and derivatives exhibit cytotoxic effects against various cancer cell lines, including HCT-116, HepG2, MCF-7, HeLa-S3, PANC-1, ECA-109, SF-295, OVCAR-8, U87-MG, U251, and Caco-2 [119].

In this study, the presence of cyclo(D-Phe-L-Pro) and cyclo(L-Leu-L-Pro) was confirmed by GC-MS using the DMSO derivatization of CFS (Fig. S4 and Table S6). The detected compound list belonging to the CFS of the DY55bre dissolved in acetonitrile is shared in Table S5. In addition, the literature points out that proline-based cyclic dipeptides can display a variety of features, including anticancer, antioxidant, neuroprotective, antiviral, antibacterial, anti-inflammatory, antihyperglycemic, antiarrhythmic, immunomodulatory, antiparasitic, anthelmintic, insecticidal, and metabolic regulatory activities, contingent upon their structure and application [120–124]. Therefore, the activation of apoptosis and cytotoxic effects on HT-29 and DLD-1 may originate from the cyclic dipeptides in the CFS (Fig. 9G and F). Similar cyclic dipeptide structures were previously observed in the CFS of *Lactiplantibacillus plantarum* MiLAB 393 by Ström et al. [125]. In another study by Axel et al. [126] using HRGC/MS and stable isotope dilution assay, *Lvb. brevis* R2Δ was shown to produce significant amounts ($p > 0.05$) of the cyclic dipeptides cyclo(Leu-Pro), cyclo(Pro-Pro), and cyclo(Phe-Pro), thus confirming the findings of the present study.

In general, the biosynthetic pathways of cyclic dipeptides can be classified into non-enzymatic and enzymatic mechanisms [127]. An example of the non-enzymatic pathway is the cyclization of the tripeptide His-Pro-Gly into cyclo(His-Pro), in which the presence of proline imposes conformational constraints that favor the cis-configuration of the peptide bond between histidine and proline. This conformation facilitates intramolecular cyclization, leading to the formation of the cyclic dipeptide scaffold [128]. Notably, both cyclic dipeptides detected in this study contain proline residues, suggesting that they may be biosynthesized via non-enzymatic mechanisms. In contrast, enzymatic pathways involve the action of various enzymes. Proteases, such as dipeptidyl peptidases, can cleave terminal residues of a protein to generate dipeptides, which may then undergo spontaneous cyclization. Additionally, non-ribosomal peptide synthetases (NRPSs) and cyclic dipeptide synthetases (CDPSs) are known to directly catalyze the formation of cyclic dipeptides [127]. No NRPS biosynthetic gene clusters were identified in the genome of *Lvb. brevis* strain DY55bre. However, CDPSs represent a recently characterized family of tRNA-dependent enzymes that catalyze peptide bond formation without requiring charged amino acids. These enzymes share structural homology with the catalytic domains of class-Ic aminoacyl-tRNA synthetases [129]. Therefore, the biosynthesis of the cyclic dipeptides detected in *Lvb. brevis* DY55bre may also be attributed to the activity of tRNA synthetases encoded in the genome, such as phenylalanyl-tRNA synthetase (EC 6.1.1.20) and prolyl-tRNA synthetase (EC 6.1.1.15). Furthermore, cyclic dipeptide biosynthesis is often associated with tailoring enzymes, such as cytochrome oxidases, α-ketoglutarate/Fe(II)-dependent oxygenases, various C-, N-, and O-methyltransferases, α/β-hydrolases, peptide ligases, and acyl-CoA transferases [130]. The presence of cytochrome bd ubiquinol oxidase (EC 7.1.1.7) in the *Lvb. brevis* DY55bre genome further enhances the biosynthesis of cyclic dipeptides in *Lvb. brevis* DY55bre. These inferences need to be confirmed experimentally.

Based on antibiogram results, the CFS of DY55bre showed apparent inhibition zones (> 13 mm) versus *E. coli* ATCC 25922, *E. coli* O157:H7 ATCC 43897, *B. cereus* ATCC 33019, *S. enterica* sv. typhimurium ATCC 14028, *P. mirabilis* ATCC 29906, and *E. cloacae* ATCC 13047 (Table 2). This effect might derive from 8 × concentrated CFS, which possesses 8 × higher amounts of cyclic dipeptides, organic acids, and 1,4-diaza-2,5-dioxo-3-isobutyl bicyclo[4.3.0] nonane molecules that could have a synergistic antibacterial effect against the tested pathogens. Cyclic dipeptides with at least one D-stereoisomer had significantly enhanced antibacterial properties compared to those with L-stereoisomers [131]. Thus, it is reasonable that cyclo (D-Phe-L-Pro), synthesized by the *Lvb. brevis* DY55bre strain, has significantly more antimicrobial activity than cyclo (L-Leu-L-Pro). Besides, 1,4-diaza-2,5-dioxo-3-isobutyl bicyclo[4.3.0] nonane was documented to possess antibacterial properties, demonstrating activity against multi-drug-resistant *K. pneumoniae*, *S. aureus* ATCC 25923, and *E. coli* ATCC 25922; hence, it is plausible to infer that this molecule may exhibit antimicrobial activity against the pathogens [132–134].

Antioxidant Activities

Oxidative stress is a primary factor contributing to aging and the development of age-related illnesses. In this context, the antioxidant properties of bacteria known as probiotics are becoming increasingly important due to their direct health benefits. Moreover, probiotic *Lactobacillus* strains have been proven to have a variety of antioxidant and immunomodulatory effects on the host. The antioxidant screening results revealed $ABTS^+$ and DPPH inhibitions of $76.63 \pm 0.4225\%$ and $34.25 \pm 0.3951\%$, respectively (Table 2). $ABTS^+$ and DPPH are widely recognized free radicals commonly employed to test antioxidants' free radical scavenging activities and can be assayed calorimetrically. This work suggests

that the greater ability of DY55bre to inhibit ABTS compared to DPPH inhibition may be attributed to the stronger affinity of secondary metabolites or organic acids generated by the bacteria towards ABTS than DPPH.

Furthermore, antioxidant capacity can also be associated with antioxidant enzymes, such as glutathione peroxidase (*gpx*), glutathione reductase (*gsr*), glutaredoxin-like protein NrdH, manganese transport protein, NADH dehydrogenase (*ndh*), NADH peroxidase (*npx*), pyruvate oxidase (*poxL*), thiol peroxidase (*tpx*), thioredoxin (*trxA*), thioredoxin reductase (trxB), peptide-methionine (S)-S-oxide reductase (*MsrA* and *MsrB*), and arsenate reductase (*ArsC*). Besides, these enzymes not only enhance the antioxidant capacity but also promote the survival of the strain. Lactobacilli with a whole thioredoxin system (*tpx*, *trxA*, *trxB*) can eliminate reactive-oxygen-species (ROS) and reactive-nitrogen-species at greater rates by providing electrons to thiol-dependent peroxidases [135]. The glutathione system regulates the protein dithiol/disulfide balance to detoxify radicals such as hydrogen and lipid peroxide [136]. The NADH oxidase/peroxidase and pyruvate oxidase (*poxL*) have a direct role in the breakdown of hydrogen peroxide and ROS [137]. Notably, the functions of the *msrA* and *msrB* genes are associated with restoring ROS-damaged proteins containing oxidized methionine residues [111]. Copy numbers of antioxidant enzymes show differences strain to strain depending on the isolation niche. We summarized and compared the copy numbers of probiotic and antioxidant genes in the Supplemental Excel sheet for Probiotic traits. Furthermore, the antioxidant capacity may be linked to organic acids generated by DY55bre, such as lactic acid (D-, L-), propanoic acid, butanoic acid, and cyclic dipeptides [13, 119].

Cholesterol Removal Capacity

Lactobacilli can decrease lipids and cholesterol levels in the blood through different mechanisms. High lipid and cholesterol levels in the blood (hypercholesterolemia) are associated with cardiovascular diseases, which are leading to 2.6 million deaths and 29.7 million disability-adjusted Life years based on the WHO 2024 Global Patient Safety Report. Therefore, enrichment of foods with lactic acid bacteria or direct consumption of probiotics has gained significance due to growing cardiovascular health concerns [138, 139]. In this case, comparable cholesterol-lowering effects were detected in vitro for this study. According to cholesterol assimilation test results, DY55bre has been used $27.28843 \pm 0.82\%$ of 100 ppm cholesterol for 24 h (Table 2). In previous studies, 2.7%, 4.8%, 5.2%, 7.7%, 10.5%, 59.1%, 59.8%, and 62.8% cholesterol removal for *Lvb. brevis* 119-6, NBRC3345, NBRC13110, NBRC12005, NBRC12520, NBRC13109, NBRC3960, and 119-2 strains, respectively [140]. Another research reported that the cholesterol removal rate for *Lvb. brevis* CH7 was close to 30% [141].

The molecular mechanism underlying the hypocholesterolemic effects is often attributed to the presence of bile salt hydrolase (*bsh* or *cbh*) enzymes or the synthesis of short-chain fatty acids, which inhibit enzymes such as 3-hydroxy-3-methylglutaryl coenzyme A (HMB-CoA). This enzyme catalyzes mevalonic acid synthesis, a crucial step in cholesterol biosynthesis in humans and animals [138, 142]. The choloylglycine hydrolase (*cbh*) enzyme was validated with bile salt hydrolase-like activity via in silico approaches. In addition, DY55bre possesses three copies of both genes, with the specific copy number of each gene varying among strains, as detailed in the Supplemental Excel sheet for Probiotic traits.

Conclusion

The present study provides a thorough genetic, metabolic, and probiotic assessment of *Lvb. brevis* DY55bre, a strain derived from the traditional Turkish fermented drink Shalgam. Bioinformatic analyses revealed that the DY55bre strain had a circular genome of 2.485 Mb, with a GC content of 45.72%, encoding 2699 protein-coding sequences, 82 tRNAs, and multiple CRISPR-Cas systems. The Pangenome analysis demonstrated an open structure, with 18.9% of the genes constituting the core genome and 103 strain-specific singletons belonging to the DY55bre, highlighting the genetic diversity and flexibility of *Lvb. brevis* strains. The existence of unique genes linked to carbohydrate metabolism, stress resistance, and adhesion emphasizes the potential of DY55bre for biotechnological and probiotic applications. The probiotic characterization of DY55bre showed its firm survival in simulated gastrointestinal conditions, including resistance to low pH (as low as 3.0) and bile salts (up to 1%), along with its capacity to adhere to intestinal epithelial cell lines (HT29, Caco-2, and DLD-1).

The strain demonstrated significant auto-aggregation (84.55%) and cell surface hydrophobicity (56.69%), essential for colonization and persistence in the gastrointestinal system. Moreover, the strain's non-hemolytic characteristics and lack of horizontally acquired antibiotic resistance genes affirm its safety for potential probiotic applications. This study's principal finding is the biosynthesis of bioactive cyclic dipeptides, specifically cyclo(D-Phe-L-Pro) and cyclo(L-Leu-L-Pro), identified via GC-MS analysis. These compounds demonstrated considerable cytotoxicity against colorectal cancer cell lines, with IC50 values of 7.71 mg/mL for HT29 cells and 3.19 mg/mL for DLD-1 cells, indicating their potential as anticancer agents. The strain's cell-free supernatant exhibited antimicrobial activity against various pathogens, presumably attributable to the synergistic

effects of cyclic dipeptides, organic acids, and other secondary metabolites such as 1,4-diaza-2,5-dioxo-3-isobutyl bicyclo[4.3.0] nonane. The antioxidant efficacy of DY55bre, demonstrated by $ABTS^+$ (76.63%) and DPPH (34.25%) radical scavenging activity, reinforces its potential in alleviating oxidative stress-related conditions. The strain demonstrated a cholesterol removal capacity of 27.29%, potentially contributing to its hypocholesterolemic effects. This process is probably facilitated by bile salt hydrolase (like *cbh*) enzymes and the generation of short-chain fatty acids, which are recognized for their ability to inhibit cholesterol manufacturing pathways.

In summary, *Lvb. brevis* DY55bre exhibits a distinctive combination of genetic, metabolic, and probiotic characteristics, making it a promising candidate for functional foods, nutraceuticals, and medicinal applications. Its capacity to generate bioactive molecules with anticancer, antibacterial, antioxidant, and cholesterol-lowering attributes underscores its potential to tackle significant health issues like cancer, cardiovascular disorders, and gut dysbiosis. The possibility for strain engineering through its native CRISPR-Cas system presents promising options for improving its functional features and broadening its applications in the food and pharmaceutical sectors.

Supplementary Information The online version contains supplementary material available at https://doi.org/10.1007/s12602-025-10760-7.

Acknowledgements We would like to thank the Proofreading & Editing Office of the Dean for Research at Erciyes University for the copyediting and proofreading service for this manuscript.

Author Contribution All authors contributed to the study's conception and design. Material preparation, data collection, and analysis were performed by Ahmet E. Yetiman, Mehmet Horzum, Ertan Kanbur, Mehmet Çadır, Şerife Gürbüz, Dilek Bahar, Melisa Z. Karaman, Özkan Fidan, Murat Kaya, and Sevda Yetiman. The first draft of the manuscript was written by Ahmet E. Yetiman and Sevda Yetiman and was proofread by Mikail Akbulut and Mahmut Doğan. All authors read and approved the final manuscript.

Funding This study has been financially supported by Erciyes University Scientific Research Projects Coordination Unit under grant number FBA-2025-14779.

Data Availability No datasets were generated or analysed during the current study.

Declarations

Conflict of interest The authors declare no competing interests.

References

1. Feyereisen M, Mahony J, Kelleher P, Roberts RJ, O'Sullivan T, Geertman JA, van Sinderen D (2019) Comparative genome analysis of the Lactobacillus brevis species. BMC Genomics 20(1):416. https://doi.org/10.1186/s12864-019-5783-1
2. Buron-Moles G, Chailyan A, Dolejs I, Forster J, Miks MH (2019) Uncovering carbohydrate metabolism through a genotype-phenotype association study of 56 lactic acid bacteria genomes. Appl Microbiol Biotechnol 103(7):3135–3152. https://doi.org/10.1007/s00253-019-09701-6
3. Jeon JH, Kim JS, Kim ZH, Jung JY. Complete genome sequence of Levilactobacillus brevis NSMJ23, makgeolli isolate with antimicrobial activity. Microbiol Resour Announc. 2024:e0106023. https://doi.org/10.1128/mra.01060-23.
4. Kwun SY, Yoon JA, Kim GY, Bae YW, Park EH, Kim MD (2024) Isolation of a potential probiotic Levilactobacillus brevis and evaluation of its exopolysaccharide for antioxidant and alpha-glucosidase inhibitory activities. J Microbiol Biotechnol 34(1):167–175. https://doi.org/10.4014/jmb.2304.04043
5. Somashekaraiah R, Mottawea W, Gunduraj A, Joshi U, Hammami R, Sreenivasa MY (2021) Probiotic and antifungal attributes of *Levilactobacillus brevis* MYSN105, isolated from an Indian traditional fermented food Pozha. Front Microbiol 12. https://doi.org/10.3389/fmicb.2021.696267
6. Hojjati M, Behabahani BA, Falah F (2020) Aggregation, adherence, anti-adhesion and antagonistic activity properties relating to surface charge of probiotic *Lactobacillus brevis* gp104 against *Staphylococcus aureus*. Microb Pathog 147. https://doi.org/10.1016/j.micpath.2020.104420
7. Kim WJ, Hyun JH, Lee NK, Paik HD (2022) Protective effects of a novel *Lactobacillus brevis* strain with probiotic characteristics against *Staphylococcus aureus* lipoteichoic acid-induced intestinal inflammatory response. J Microbiol Biotechnol 32(2):205–211. https://doi.org/10.4014/jmb.2110.10034
8. Ogawa M, Saiki A, Matsui Y, Tsuchimoto N, Nakakita Y, Takata Y, Nakamura T (2016) Effects of oral intake of heat-killed *Lactobacillus brevis* SBC8803 (SBL88) on dry skin conditions: a randomized, double-blind, placebo-controlled study. Exp Ther Med 12(6):3863–3872. https://doi.org/10.3892/etm.2016.3862
9. Watanabe J, Hashimoto N, Yin T, Sandagdorj B, Arakawa C, Inoue T, Suzuki S (2021) Heat-killed *Lactobacillus brevis* KB290 attenuates visceral fat accumulation induced by high-fat diet in mice. J Appl Microbiol 131(4):1998–2009. https://doi.org/10.1111/jam.15079
10. Okada T, Sugishita T, Murakami T, Murai H, Saikusa T, Horino T et al (2000) Effect of the defatted rice germ enriched with GABA for sleeplessness, depression, autonomic disorder by oral administration. Nippon Shokuhin Kagaku Kogaku Kaishi 47(8):596–603
11. Abdou AM, Higashiguchi S, Horie K, Kim M, Hatta H, Yokogoshi H (2006) Relaxation and immunity enhancement effects of gamma-aminobutyric acid (GABA) administration in humans. BioFactors 26(3):201–208. https://doi.org/10.1002/biof.5520260305
12. Erol I, Kotil SE, Fidan O, Yetiman AE, Durdagi S, Ortakci F (2023) In silico analysis of bacteriocins from lactic acid bacteria against SARS-CoV-2. Probiotics Antimicrob Proteins 15(1):17–29. https://doi.org/10.1007/s12602-021-09879-0
13. Yetiman A, Horzum M, Bahar D, Akbulut M (2024) Assessment of genomic and metabolic characteristics of cholesterol-reducing and GABA producer Limosilactobacillus fermentum AGA52 isolated from lactic acid fermented shalgam based on "in silico" and "in vitro" approaches. Probiotics Antimicrob Proteins 16(2):334–351. https://doi.org/10.1007/s12602-022-10038-2
14. Larini I, Tintori S, Gatto V, Felis GE, Salvetti E, Torriani S (2024) Comparative genomics reveals the potential biotechnological applications of *Liquorilactobacillus nagelii* VUCC-R001, a strain isolated from kombucha tea. Food Biosci 59
15. Salvetti E, Torriani S, Felis GE (2012) The genus *Lactobacillus*: a taxonomic update. Probiotics Antimicrob Proteins 4(4):217–226. https://doi.org/10.1007/s12602-012-9117-8

16. Salvetti E, Harris HMB, Felis GE, O'Toole PW (2018) Comparative genomics of the genus *Lactobacillus* reveals robust phylogroups that provide the basis for reclassification. Appl Environ Microbiol. https://doi.org/10.1128/AEM.00993-18
17. Yetiman A. Pangenome analysis and "in silico" overview of carbohydrate and vitamin metabolism of Lactiplantibacillus plantarum strain TRA56 obtained from lactic-acid fermented beverage known as Shalgam. Biotech Studies. 2025;34(1):1–21. https://doi.org/10.38042/biotechstudies.1615601.
18. Yetiman AE, Keskin A, Darendeli BN, Kotil SE, Ortakci F, Dogan M (2022) Characterization of genomic, physiological, and probiotic features *Lactiplantibacillus plantarum* DY46 strain isolated from traditional lactic acid fermented shalgam beverage. Food Biosci 46
19. Tanguler H, Erten H (2012) Occurrence and growth of lactic acid bacteria species during the fermentation of shalgam (salgam), a traditional Turkish fermented beverage. LWT-Food Sci Technol 46(1):36–41
20. Ekinci FY, Baser GM, Özcan E, Üstündağ ÖG, Korachi M, Sofu A et al (2016) Characterization of chemical, biological, and antiproliferative properties of fermented black carrot juice, shalgam. Eur Food Res Technol 242:1355–1368
21. Agirman B, Settanni L, Erten H (2021) Effect of different mineral salt mixtures and dough extraction procedure on the physical, chemical and microbiological composition of salgam: a black carrot fermented beverage. Food Chem 344. https://doi.org/10.1016/j.foodchem.2020.128618
22. Bergsveinson J, Pittet V, Ewen E, Baecker N, Ziola B (2015) Genome sequence of rapid beer-spoiling isolate *Lactobacillus brevis* BSO 464. Genome Announc. https://doi.org/10.1128/genomeA.01411-15
23. Bergsveinson J, Ziola B (2017) Comparative genomic and plasmid analysis of beer-spoiling and non-beer-spoiling *Lactobacillus brevis* isolates. Can J Microbiol 63(12):970–983
24. Fraunhofer ME, Geissler AJ, Behr J, Vogel RF (2019) Comparative genomics of *Lactobacillus brevis* reveals a significant plasmidome overlap of brewery and insect isolates. Curr Microbiol 76(1):37–47. https://doi.org/10.1007/s00284-018-1581-2
25. Zhao Y, Wu X, Siegumfeldt H (2023) Comparative gene analysis of beer tolerant and sensitive *Lactobacillus brevis*. Food Sci Technol 43
26. Pérez-Díaz IM, Page CA, Mendez-Sandoval L, Johanningsmeier SD (2023) *Levilactobacillus brevis*, autochthonous to cucumber fermentation, is unable to utilize citric acid and encodes for a putative 1, 2-propanediol utilization microcompartment. Front Microbiol 14
27. Bolger AM, Lohse M, Usadel B (2014) Trimmomatic: a flexible trimmer for Illumina sequence data. Bioinformatics 30(15):2114–2120
28. Prjibelski A, Antipov D, Meleshko D, Lapidus A, Korobeynikov A (2020) Using SPAdes de novo assembler. Curr Protoc Bioinform 70(1)
29. Tatusova T, DiCuccio M, Badretdin A, Chetvernin V, Nawrocki EP, Zaslavsky L et al (2016) NCBI prokaryotic genome annotation pipeline. Nucleic Acids Res 44(14):6614–6624. https://doi.org/10.1093/nar/gkw569
30. Brettin T, Davis JJ, Disz T, Edwards RA, Gerdes S, Olsen GJ et al (2015) RASTtk: a modular and extensible implementation of the RAST algorithm for building custom annotation pipelines and annotating batches of genomes. Sci Rep 5. https://doi.org/10.1038/srep08365
31. Olson RD, Assaf R, Brettin T, Conrad N, Cucinell C, Davis JJ et al (2023) Introducing the bacterial and viral bioinformatics resource center (BV-BRC): a resource combining PATRIC, IRD and ViPR. Nucleic Acids Res 51(D1):D678–D689. https://doi.org/10.1093/nar/gkac1003
32. Alikhan NF, Petty NK, Ben Zakour NL, Beatson SA (2011) BLAST Ring Image Generator (BRIG): simple prokaryote genome comparisons. BMC Genomics 12:402. https://doi.org/10.1186/1471-2164-12-402
33. Seemann T (2014) Prokka: rapid prokaryotic genome annotation. Bioinformatics 30(14):2068–2069
34. Perrin A, Rocha EPC (2021) Panacota: a modular tool for massive microbial comparative genomics. NAR Genom Bioinform 3(1). https://doi.org/10.1093/nargab/lqaa106
35. Dereeper A, Summo M, Meyer DF (2022) Panexplorer: a web-based tool for exploratory analysis and visualization of bacterial pan-genomes. Bioinformatics 38(18):4412–4414. https://doi.org/10.1093/bioinformatics/btac504
36. Jain C, Rodriguez RL, Phillippy AM, Konstantinidis KT, Aluru S (2018) High throughput ANI analysis of 90K prokaryotic genomes reveals clear species boundaries. Nat Commun 9(1):5114. https://doi.org/10.1038/s41467-018-07641-9
37. Zheng J, Ge Q, Yan Y, Zhang X, Huang L, Yin Y (2023) dbCAN3: automated carbohydrate-active enzyme and substrate annotation. Nucleic Acids Res 51(W1):W115–W121
38. Couvin D, Bernheim A, Toffano-Nioche C, Touchon M, Michalik J, Néron B et al (2018) Crisprcasfinder, an update of crisrfinder, includes a portable version, enhanced performance and integrates search for Cas proteins. Nucleic Acids Res 46(W1):W246–W251
39. R-Core-Team. R: A language and environment for statistical computing. Vienna, Austria: R Foundation for Statistical Computing Retrieved from http://wwwR-projectorg 2010.
40. Kutmon M, van Iersel MP, Bohler A, Kelder T, Nunes N, Pico AR, Evelo CT (2015) Pathvisio 3: an extendable pathway analysis toolbox. PLoS Comput Biol 11(2)
41. Blin K, Shaw S, Kloosterman AM, Charlop-Powers Z, Van Wezel GP, Medema MH, Weber T. antiSMASH 6.0: improving cluster detection and comparison capabilities. Nucleic acids research. 2021;49(W1):W29-W35.
42. Brodkorb A, Egger L, Alminger M, Alvito P, Assuncao R, Ballance S et al (2019) Infogest static *in vitro* simulation of gastrointestinal food digestion. Nat Protoc 14(4):991–1014. https://doi.org/10.1038/s41596-018-0119-1
43. Krausova G, Hyrslova I, Hynstova I (2019) In vitro evaluation of adhesion capacity, hydrophobicity, and auto-aggregation of newly isolated potential probiotic strains. Fermentation 5(4)
44. Ozturk G, Yetiman AE, Dogan M (2019) The bioactive efficiency of ultrasonic extracts from acorn leaves and green walnut husks against Bacillus cereus: a hybrid approach to PCA with the Taguchi method. Journal of Food Measurement and Characterization 13:1257–1268
45. Song MW, Jang HJ, Kim KT, Paik HD (2019) Probiotic and antioxidant properties of novel *Lactobacillus brevis* KCCM 12203P isolated from kimchi and evaluation of immune-stimulating activities of its heat-killed cells in RAW 264.7 cells. J Microbiol Biotechnol 29(12):1894–1903. https://doi.org/10.4014/jmb.1907.07081
46. Yue Y, Wang S, Shi J, Xie Q, Li N, Guan J, et al. Effects of Lactobacillus acidophilus KLDS1.0901 on proliferation and apoptosis of colon cancer cells. Front Microbiol. 2021;12:788040. https://doi.org/10.3389/fmicb.2021.788040.
47. Wood PL, Khan MA, Moskal JR (2006) Neurochemical analysis of amino acids, polyamines and carboxylic acids: GC-MS quantitation of tBDMS derivatives using ammonia positive chemical ionization. J Chromatogr B Analyt Technol Biomed Life Sci 831(1–2):313–319. https://doi.org/10.1016/j.jchromb.2005.12.031
48. Rudel LL, Morris MD (1973) Determination of cholesterol using o-phthalaldehyde. J Lipid Res 14(3):364–366
49. Juhas M, van der Meer JR, Gaillard M, Harding RM, Hood DW, Crook DW (2009) Genomic islands: tools of bacterial horizontal

gene transfer and evolution. FEMS Microbiol Rev 33(2):376–393. https://doi.org/10.1111/j.1574-6976.2008.00136.x
50. Mann S, Chen YP (2010) Bacterial genomic G+C composition-eliciting environmental adaptation. Genomics 95(1):7–15. https://doi.org/10.1016/j.ygeno.2009.09.002
51. Brandt K, Nethery MA, O'Flaherty S, Barrangou R (2020) Genomic characterization of *Lactobacillus fermentum* DSM 20052. BMC Genomics 21(1):328. https://doi.org/10.1186/s12864-020-6740-8
52. Brandt K, Barrangou R. Using glycolysis enzyme sequences to inform Lactobacillus phylogeny. Microb Genom. 2018;4(6). https://doi.org/10.1099/mgen.0.000187.
53. Konstantinidis KT, Tiedje JM (2005) Genomic insights that advance the species definition for prokaryotes. Proc Natl Acad Sci U S A 102(7):2567–2572
54. Lee I, Ouk Kim Y, Park SC, Chun J (2016) OrthoANI: An improved algorithm and software for calculating average nucleotide identity. Int J Syst Evol Microbiol 66(2):1100–1103. https://doi.org/10.1099/ijsem.0.000760
55. Duar RM, Lin XB, Zheng J, Martino ME, Grenier T, Perez-Munoz ME et al (2017) Lifestyles in transition: evolution and natural history of the genus *Lactobacillus*. FEMS Microbiol Rev 41(Supp_1):S27–S48. https://doi.org/10.1093/femsre/fux030
56. Tannock GW (2004) A special fondness for lactobacilli. Appl Environ Microbiol 70(6):3189–3194. https://doi.org/10.1128/AEM.70.6.3189-3194.2004
57. Walter J (2008) Ecological role of lactobacilli in the gastrointestinal tract: implications for fundamental and biomedical research. Appl Environ Microbiol 74(16):4985–4996. https://doi.org/10.1128/AEM.00753-08
58. Barrangou R, Marraffini LA (2014) CRISPR-Cas systems: prokaryotes upgrade to adaptive immunity. Mol Cell 54(2):234–244. https://doi.org/10.1016/j.molcel.2014.03.011
59. Roberts A, Barrangou R (2020) Applications of CRISPR-Cas systems in lactic acid bacteria. FEMS Microbiol Rev 44(5):523–537. https://doi.org/10.1093/femsre/fuaa016
60. Goh YX, Wang M, Hou XP, He Y, Ou HY (2023) Analysis of CRISPR-Cas loci and their targets in *Levilactobacillus brevis*. Interdiscip Sci 15(3):349–359. https://doi.org/10.1007/s12539-023-00555-1
61. Panahi B, Majidi M, Hejazi MA (2022) Genome mining approach reveals the occurrence and diversity pattern of clustered regularly interspaced short palindromic repeats/CRISPR-associated systems in *Lactobacillus brevis* strains. Front Microbiol 13. https://doi.org/10.3389/fmicb.2022.911706
62. Makarova KS, Wolf YI, Iranzo J, Shmakov SA, Alkhnbashi OS, Brouns SJJ, et al (2020) Evolutionary classification of CRISPR-Cas systems: a burst of class 2 and derived variants. Nat Rev Microbiol 18(2):67–83. https://doi.org/10.1038/s41579-019-0299-x
63. Hidalgo-Cantabrana C, Goh YJ, Pan M, Sanozky-Dawes R, Barrangou R (2019) Genome editing using the endogenous type I CRISPR-Cas system in *Lactobacillus crispatus*. Proc Natl Acad Sci U S A 116(32):15774–15783. https://doi.org/10.1073/pnas.1905421116
64. Mosquera-Rendon J, Rada-Bravo AM, Cardenas-Brito S, Corredor M, Restrepo-Pineda E, Benitez-Paez A (2016) Pangenome-wide and molecular evolution analyses of the *Pseudomonas aeruginosa* species. BMC Genomics 17. https://doi.org/10.1186/s12864-016-2364-4
65. Tettelin H, Riley D, Cattuto C, Medini D (2008) Comparative genomics: the bacterial pan-genome. Curr Opin Microbiol 11(5):472–477. https://doi.org/10.1016/j.mib.2008.09.006
66. Li O, Zhang H, Wang W, Liang Y, Chen W, Din AU, et al. Complete genome sequence and probiotic properties of Lactococcus petauri LZys1 isolated from healthy human gut. J Med Microbiol. 2021;70(8). https://doi.org/10.1099/jmm.0.001397.
67. Tettelin H, Masignani V, Cieslewicz MJ, Donati C, Medini D, Ward NL et al (2005) Genome analysis of multiple pathogenic isolates of Streptococcus agalactiae: implications for the microbial "pan-genome." Proc Natl Acad Sci U S A 102(39):13950–13955. https://doi.org/10.1073/pnas.0506758102
68. Vernikos G, Medini D, Riley DR, Tettelin H (2015) Ten years of pan-genome analyses. Curr Opin Microbiol 23:148–154. https://doi.org/10.1016/j.mib.2014.11.016
69. Mendonca AG, Alves RJ, Pereira-Leal JB (2011) Loss of genetic redundancy in reductive genome evolution. PLoS Comput Biol 7(2). https://doi.org/10.1371/journal.pcbi.1001082
70. McInerney JO, McNally A, O'Connell MJ (2017) Why prokaryotes have pangenomes. Nat Microbiol 2. https://doi.org/10.1038/nmicrobiol.2017.40
71. Fagan RP, Fairweather NF (2014) Biogenesis and functions of bacterial S-layers. Nat Rev Microbiol 12(3):211–222. https://doi.org/10.1038/nrmicro3213
72. Gerbino E, Carasi P, Mobili P, Serradell MA, Gomez-Zavaglia A (2015) Role of S-layer proteins in bacteria. World J Microbiol Biotechnol 31(12):1877–1887. https://doi.org/10.1007/s11274-015-1952-9
73. Klotz C, Goh YJ, O'Flaherty S, Barrangou R (2020) S-layer associated proteins contribute to the adhesive and immunomodulatory properties of Lactobacillus acidophilus NCFM. BMC Microbiol 20(1):248. https://doi.org/10.1186/s12866-020-01908-2
74. Lucas PM, Blancato VS, Claisse O, Magni C, Lolkema JS, Lonvaud-Funel A (2007) Agmatine deiminase pathway genes in *Lactobacillus brevis* are linked to the tyrosine decarboxylation operon in a putative acid resistance locus. Microbiology (Reading) 153(Pt 7):2221–2230. https://doi.org/10.1099/mic.0.2007/006320-0
75. Papadimitriou K, Alegria A, Bron PA, de Angelis M, Gobbetti M, Kleerebezem M et al (2016) Stress physiology of lactic acid bacteria. Microbiol Mol Biol Rev 80(3):837–890. https://doi.org/10.1128/MMBR.00076-15
76. Okamoto S, Tamaru A, Nakajima C, Nishimura K, Tanaka Y, Tokuyama S et al (2007) Loss of a conserved 7-methylguanosine modification in 16S rRNA confers low-level streptomycin resistance in bacteria. Mol Microbiol 63(4):1096–1106. https://doi.org/10.1111/j.1365-2958.2006.05585.x
77. Alcock BP, Raphenya AR, Lau TTY, Tsang KK, Bouchard M, Edalatmand A et al (2020) CARD 2020: antibiotic resistome surveillance with the comprehensive antibiotic resistance database. Nucleic Acids Res 48(D1):D517–D525. https://doi.org/10.1093/nar/gkz935
78. Alcock BP, Huynh W, Chalil R, Smith KW, Raphenya AR, Wlodarski MA et al (2023) CARD 2023: expanded curation, support for machine learning, and resistome prediction at the comprehensive antibiotic resistance database. Nucleic Acids Res 51(D1):D690–D699. https://doi.org/10.1093/nar/gkac920
79. Theron MM, Janse Van Rensburg MN, Chalkley LJ. Nitroimidazole resistance genes (nimB) in anaerobic Gram-positive cocci (previously Peptostreptococcus spp.). J Antimicrob Chemother. 2004;54(1):240–2. https://doi.org/10.1093/jac/dkh270.
80. Douthwaite S, Jakobsen L, Yoshizawa S, Fourmy D (2008) Interaction of the tylosin-resistance methyltransferase RlmA II at its rRNA target differs from the orthologue RlmA I. J Mol Biol 378(5):969–975. https://doi.org/10.1016/j.jmb.2008.03.024
81. Zhu L, Lin J, Ma J, Cronan JE, Wang H (2010) Triclosan resistance of *Pseudomonas aeruginosa* PAO1 is due to FabV, a triclosan-resistant enoyl-acyl carrier protein reductase. Antimicrob Agents Chemother 54(2):689–698. https://doi.org/10.1128/AAC.01152-09

82. Jack DL, Storms ML, Tchieu JH, Paulsen IT, Saier MH (2000) A broad-specificity multidrug efflux pump requiring a pair of homologous SMR-type proteins. J Bacteriol 182(8):2311–2313. https://doi.org/10.1128/JB.182.8.2311-2313.2000
83. Friedman L, Alder JD, Silverman JA (2006) Genetic changes that correlate with reduced susceptibility to daptomycin in *Staphylococcus aureus*. Antimicrob Agents Chemother 50(6):2137–2145. https://doi.org/10.1128/AAC.00039-06
84. Yang SJ, Xiong YQ, Dunman PM, Schrenzel J, Francois P, Peschel A, Bayer AS (2009) Regulation of mprF in daptomycin-nonsusceptible Staphylococcus aureus strains. Antimicrob Agents Chemother 53(6):2636–2637. https://doi.org/10.1128/AAC.01415-08
85. Abriouel H, Casado Munoz MDC, Lavilla Lerma L, Perez Montoro B, Bockelmann W, Pichner R et al (2015) New insights in antibiotic resistance of *Lactobacillus* species from fermented foods. Food Res Int 78:465–481. https://doi.org/10.1016/j.foodres.2015.09.016
86. Zheng M, Zhang R, Tian X, Zhou X, Pan X, Wong A (2017) Assessing the risk of probiotic dietary supplements in the context of antibiotic resistance. Front Microbiol 8. https://doi.org/10.3389/fmicb.2017.00908
87. Hazards EPoB, Koutsoumanis K, Allende A, Alvarez-Ordonez A, Bolton D, Bover-Cid S, et al. Statement on how to interpret the QPS qualification on "acquired antimicrobial resistance genes'. EFSA J. 2023;21(10):e08323. https://doi.org/10.2903/j.efsa.2023.8323.
88. Gueimonde M, Sanchez B, C GdLR-G, Margolles A. Antibiotic resistance in probiotic bacteria. Front Microbiol. 2013;4:202. https://doi.org/10.3389/fmicb.2013.00202.
89. Yetiman AE, Ortakci F (2023) Genomic, probiotic, and metabolic potentials of *Liquorilactobacillus nagelii* AGA58, a novel bacteriocinogenic motile strain isolated from lactic acid-fermented shalgam. J Biosci Bioeng 135(1):34–43. https://doi.org/10.1016/j.jbiosc.2022.10.008
90. Ganzle MG, Follador R (2012) Metabolism of oligosaccharides and starch in lactobacilli: a review. Front Microbiol 3. https://doi.org/10.3389/fmicb.2012.00340
91. Kleerebezem M, Boekhorst J, van Kranenburg R, Molenaar D, Kuipers OP, Leer R et al (2003) Complete genome sequence of *Lactobacillus plantarum* WCFS1. Proc Natl Acad Sci U S A 100(4):1990–1995. https://doi.org/10.1073/pnas.0337704100
92. Pessione E (2012) Lactic acid bacteria contribution to gut microbiota complexity: lights and shadows. Front Cell Infect Microbiol 2. https://doi.org/10.3389/fcimb.2012.00086
93. Thomas LM, Harper AR, Miner WA, Ajufo HO, Branscum KM, Kao L, Sims PA (2013) Structure of *Escherichia coli* AdhP (ethanol-inducible dehydrogenase) with bound NAD. Acta Crystallogr Sect F Struct Biol Cryst Commun 69(Pt 7):730–732. https://doi.org/10.1107/S1744309113015170
94. Garcia-Quintans N, Repizo G, Martin M, Magni C, Lopez P. Activation of the diacetyl/acetoin pathway in Lactococcus lactis subsp. lactis bv. diacetylactis CRL264 by acidic growth. Appl Environ Microbiol. 2008;74(7):1988–96. https://doi.org/10.1128/AEM.01851-07.
95. Takusagawa Y, Otagiri M, Ui S, Ohtsuki T, Mimura A, Ohkuma M, Kudo T (2001) Purification and characterization of L-2,3-butanediol dehydrogenase of *Brevibacterium saccharolyticum* C-1012 expressed in *Escherichia coli*. Biosci Biotechnol Biochem 65(8):1876–1878. https://doi.org/10.1271/bbb.65.1876
96. Morita H, Toh H, Fukuda S, Horikawa H, Oshima K, Suzuki T et al (2008) Comparative genome analysis of *Lactobacillus reuteri* and *Lactobacillus fermentum* reveal a genomic island for reuterin and cobalamin production. DNA Res 15(3):151–161. https://doi.org/10.1093/dnares/dsn009
97. Bobik TA, Havemann GD, Busch RJ, Williams DS, Aldrich HC (1999) The propanediol utilization (pdu) operon of *Salmonella enterica* serovar typhimurium LT2 includes genes necessary for formation of polyhedral organelles involved in coenzyme B(12)-dependent 1, 2-propanediol degradation. J Bacteriol 181(19):5967–5975. https://doi.org/10.1128/JB.181.19.5967-5975.1999
98. Dishisha T, Pereyra LP, Pyo SH, Britton RA, Hatti-Kaul R (2014) Flux analysis of the *Lactobacillus reuteri* propanediol-utilization pathway for production of 3-hydroxypropionaldehyde, 3-hydroxypropionic acid and 1,3-propanediol from glycerol. Microb Cell Fact 13. https://doi.org/10.1186/1475-2859-13-76
99. Mohan CD, Rangappa S, Nayak SC, Jadimurthy R, Wang L, Sethi G et al (2022) Bacteria as a treasure house of secondary metabolites with anticancer potential. Semin Cancer Biol 86(Pt 2):998–1013. https://doi.org/10.1016/j.semcancer.2021.05.006
100. Yamada Y, Kuzuyama T, Komatsu M, Shin-Ya K, Omura S, Cane DE, Ikeda H (2015) Terpene synthases are widely distributed in bacteria. Proc Natl Acad Sci U S A 112(3):857–862. https://doi.org/10.1073/pnas.1422108112
101. Theisen MJ, Misra I, Saadat D, Campobasso N, Miziorko HM, Harrison DH (2004) 3-Hydroxy-3-methylglutaryl-CoA synthase intermediate complex observed in "real-time." Proc Natl Acad Sci U S A 101(47):16442–16447. https://doi.org/10.1073/pnas.0405809101
102. Zhang Q, Yu Y, Velasquez JE, van der Donk WA (2012) Evolution of lanthipeptide synthetases. Proc Natl Acad Sci U S A 109(45):18361–18366. https://doi.org/10.1073/pnas.1210393109
103. Bruna P, Nunez-Montero K, Contreras MJ, Leal K, Garcia M, Abanto M, Barrientos L (2024) Biosynthetic gene clusters with biotechnological applications in novel Antarctic isolates from Actinomycetota. Appl Microbiol Biotechnol 108(1). https://doi.org/10.1007/s00253-024-13154-x
104. Haddad MJ, Sztupecki W, Delayre-Orthez C, Rhazi L, Barbezier N, Depeint F, Anton PM (2023) Complexification of *in vitro* models of intestinal barriers, a true challenge for a more accurate alternative approach. Int J Mol Sci. https://doi.org/10.3390/ijms24043595
105. Sun Y, Zhang S, Li H, Zhu J, Liu Z, Hu X, Yi J (2022) Assessments of probiotic potentials of *Lactiplantibacillus plantarum* strains isolated from Chinese traditional fermented food: phenotypic and genomic analysis. Front Microbiol 13. https://doi.org/10.3389/fmicb.2022.895132
106. de Souza BMS, Borgonovi TF, Casarotti SN, Todorov SD, Penna ALB (2019) *Lactobacillus casei* and *Lactobacillus fermentum* strains isolated from mozzarella cheese: probiotic potential, safety, acidifying kinetic parameters and viability under gastrointestinal tract conditions. Probiotics Antimicrob Proteins 11(2):382–396. https://doi.org/10.1007/s12602-018-9406-y
107. Del Re B, Sgorbati B, Miglioli M, Palenzona D (2000) Adhesion, autoaggregation and hydrophobicity of 13 strains of *Bifidobacterium longum*. Lett Appl Microbiol 31(6):438–442. https://doi.org/10.1046/j.1365-2672.2000.00845.x
108. Rajoka MSR, Mehwish HM, Siddiq M, Haobin Z, Zhu J, Yan L et al (2017) Identification, characterization, and probiotic potential of *Lactobacillus rhamnosus* isolated from human milk. LWT 84:271–280
109. Brown S, Santa Maria JP Jr., Walker S (2013) Wall teichoic acids of gram-positive bacteria. Annu Rev Microbiol 67:313–336. https://doi.org/10.1146/annurev-micro-092412-155620
110. He Z, Liang J, Tang Z, Ma R, Peng H, Huang Z (2015) Role of the luxS gene in initial biofilm formation by Streptococcus mutans. J Mol Microbiol Biotechnol 25(1):60–68. https://doi.org/10.1159/000371816
111. Kandasamy S, Yoo J, Yun J, Lee KH, Kang HB, Kim JE et al (2022) Probiogenomic *in-silico* analysis and safety assessment

of *Lactiplantibacillus plantarum* DJF10 strain isolated from Korean raw milk. Int J Mol Sci. https://doi.org/10.3390/ijms232214494
112. Ouwehand AC, Kirjavainen PV, Shortt C, Salminen S (1999) Probiotics: mechanisms and established effects. Int Dairy J 9(1):43–52
113. Hill C, Guarner F, Reid G, Gibson GR, Merenstein DJ, Pot B et al (2014) The international scientific association for probiotics and prebiotics consensus statement on the scope and appropriate use of the term probiotic. Nat Rev Gastroenterol Hepatol 11(8):506–514. https://doi.org/10.1038/nrgastro.2014.66
114. Behbahani BA, Jooyandeh H, Hojjati M, Sheikhjan MG (2024) Evaluation of probiotic, safety, and anti-pathogenic properties of Levilactobacillus brevis HL6, and its potential application as bio-preservatives in peach juice. Lwt 191
115. Saarela M, Mogensen G, Fonden R, Mättö J, Mattila-Sandholm T (2000) Probiotic bacteria: safety, functional and technological properties. J Biotechnol 84(3):197–215
116. Zhang L, Ma H, Kulyar MF-e-A, Pan H, Li K, Li A, et al. Complete genome analysis of Lactobacillus fermentum YLF016 and its probiotic characteristics. Microbial Pathogenesis. 2022;162:105212.
117. Gao Y, Liu Y, Sun M, Zhang H, Mu G, Tuo Y (2020) Physiological function analysis of *Lactobacillus plantarum* Y44 based on genotypic and phenotypic characteristics. J Dairy Sci 103(7):5916–5930
118. Pan DD, Zeng XQ, Yan YT (2011) Characterisation of *Lactobacillus fermentum* SM-7 isolated from koumiss, a potential probiotic bacterium with cholesterol-lowering effects. J Sci Food Agric 91(3):512–518. https://doi.org/10.1002/jsfa.4214
119. Bojarska J, Mieczkowski A, Ziora ZM, Skwarczynski M, Toth I, Shalash AO et al (2021) Cyclic dipeptides: the biological and structural landscape with special focus on the anti-cancer proline-based scaffold. Biomolecules. https://doi.org/10.3390/biom11101515
120. Falorni M, Giacomelli G, Porcheddu A, Taddei M (2000) Solution-phase synthesis of mixed amide libraries by simultaneous addition of functionalities (SPSAF) to a diketopiperazine tetracarboxylic acid scaffold monitored by GC analysis of isobutyl alcohol. Eur J Org Chem 2000(8):1669–1675
121. Martins MB, Carvalho I (2007) Diketopiperazines: biological activity and synthesis. Tetrahedron 63(40):9923–9932
122. Harizani M, Katsini E, Georgantea P, Roussis V, Ioannou E (2020) New chlorinated 2,5-diketopiperazines from marine-derived bacteria isolated from sediments of the Eastern Mediterranean Sea. Molecules. https://doi.org/10.3390/molecules25071509
123. Cornacchia C, Cacciatore I, Baldassarre L, Mollica A, Feliciani F, Pinnen F (2012) 2,5-diketopiperazines as neuroprotective agents. Mini Rev Med Chem 12(1):2–12. https://doi.org/10.2174/138955712798868959
124. Wang Y, Wang P, Ma H, Zhu W (2013) Developments around the bioactive diketopiperazines: a patent review. Expert Opin Ther Pat 23(11):1415–1433. https://doi.org/10.1517/13543776.2013.828036
125. Ström K, Sjogren J, Broberg A, Schnurer J (2002) Lactobacillus plantarum MiLAB 393 produces the antifungal cyclic dipeptides cyclo(L-Phe-L-Pro) and cyclo(L-Phe-trans-4-OH-L-Pro) and 3-phenyllactic acid. Appl Environ Microbiol 68(9):4322–4327. https://doi.org/10.1128/AEM.68.9.4322-4327.2002
126. Axel C, Zannini E, Arendt EK, Waters DM, Czerny M (2014) Quantification of cyclic dipeptides from cultures of *Lactobacillus brevis* R2Delta by HRGC/MS using stable isotope dilution assay. Anal Bioanal Chem 406(9–10):2433–2444. https://doi.org/10.1007/s00216-014-7620-3
127. Mishra AK, Choi J, Choi SJ, Baek KH (2017) Cyclodipeptides: an overview of their biosynthesis and biological activity. Molecules. https://doi.org/10.3390/molecules22101796
128. Minelli A, Bellezza I, Grottelli S, Galli F (2008) Focus on cyclo(His-Pro): history and perspectives as antioxidant peptide. Amino Acids 35(2):283–289. https://doi.org/10.1007/s00726-007-0629-6
129. Sauguet L, Moutiez M, Li Y, Belin P, Seguin J, Le Du MH et al (2011) Cyclodipeptide synthases, a family of class-I aminoacyl-tRNA synthetase-like enzymes involved in non-ribosomal peptide synthesis. Nucleic Acids Res 39(10):4475–4489. https://doi.org/10.1093/nar/gkr027
130. Giessen TW, Marahiel MA (2015) Rational and combinatorial tailoring of bioactive cyclic dipeptides. Front Microbiol 6. https://doi.org/10.3389/fmicb.2015.00785
131. Fdhila F, Vazquez V, Sanchez JL, Riguera R (2003) Dd-diketopiperazines: antibiotics active against *Vibrio anguillarum* isolated from marine bacteria associated with cultures of *Pecten maximus*. J Nat Prod 66(10):1299–1301. https://doi.org/10.1021/np030233e
132. Samirana PO, Murti YB, Jenie RI, Setyowati EP (2023) GC-MS metabolomic approach to study antimicrobial activity of the marine sponge-derived fungi Trichoderma reesei TV221. Journal of Applied Pharmaceutical Science 13(7):159–173
133. Rajivgandhi GN, Ramachandran G, Kanisha CC, Li J-L, Yin L, Manoharan N, et al. Anti-biofilm compound of 1, 4-diaza-2, 5-dioxo-3-isobutyl bicyclo [4.3. 0] nonane from marine Nocardiopsis sp. DMS 2 (MH900226) against biofilm forming K. pneumoniae. Journal of King Saud University-Science. 2020;32(8):3495–502.
134. Rajivgandhi G, Ramachandran G, Maruthupandy M, Vaseeharan B, Manoharan N (2019) Molecular identification and structural characterization of marine endophytic actinomycetes *Nocardiopsis* sp. GRG 2 (KT 235641) and its antibacterial efficacy against isolated ESBL producing bacteria. Microb Pathog 126:138–148. https://doi.org/10.1016/j.micpath.2018.10.014
135. Lu J, Holmgren A (2014) The thioredoxin antioxidant system. Free Radic Biol Med 66:75–87. https://doi.org/10.1016/j.freeradbiomed.2013.07.036
136. Pophaly SD, Singh R, Pophaly SD, Kaushik JK, Tomar SK (2012) Current status and emerging role of glutathione in food grade lactic acid bacteria. Microb Cell Fact 11. https://doi.org/10.1186/1475-2859-11-114
137. Zhang W, Ji H, Zhang D, Liu H, Wang S, Wang J, Wang Y (2018) Complete genome sequencing of *Lactobacillus plantarum* ZLP001, a potential probiotic that enhances intestinal epithelial barrier function and defense against pathogens in pigs. Front Physiol 9. https://doi.org/10.3389/fphys.2018.01689
138. Agolino G, Pino A, Vaccalluzzo A, Cristofolini M, Solieri L, Caggia C, Randazzo CL (2024) Bile salt hydrolase: the complexity behind its mechanism in relation to lowering-cholesterol lactobacilli probiotics. J Funct Foods 120
139. Zhao X, Zhong X, Liu X, Wang X, Gao X (2021) Therapeutic and improving function of Lactobacilli in the prevention and treatment of cardiovascular-related diseases: a novel perspective from gut microbiota. Front Nutr 8. https://doi.org/10.3389/fnut.2021.693412
140. Watanabe S, Katsube T, Hattori H, Sato H, Ishijima T, Nakai Y et al (2013) Effect of *Lactobacillus brevis* 119–2 isolated from Tsuda kabu red turnips on cholesterol levels in cholesterol-administered rats. J Biosci Bioeng 116(1):45–51. https://doi.org/10.1016/j.jbiosc.2013.01.009
141. Song M, Yun B, Moon JH, Park DJ, Lim K, Oh S (2015) Characterization of selected *Lactobacillus* strains for use as probiotics. Korean J Food Sci Anim Resour 35(4):551–556. https://doi.org/10.5851/kosfa.2015.35.4.551

142. Wilson JM, Fitschen PJ, Campbell B, Wilson GJ, Zanchi N, Taylor L et al (2013) International society of sports nutrition position stand: beta-hydroxy-beta-methylbutyrate (HMB). J Int Soc Sports Nutr 10(1). https://doi.org/10.1186/1550-2783-10-6